SIMPL Greenland 2015 Campaign

Release 5 Data Product Documentation and Instrument Description

SIMPL TEAM
David Harding, Principal Investigator
Philip Dabney, Instrument Scientist and System Engineer
Susan Valett, Lead Software Engineer Lead
Anthony Yu, Electro-optical Physicist and Transmitter Lead
Kurt Rush, Electronics Engineer Lead
Beth Timmons, Software Engineer
Gerry McIntire, Mechanical Engineer
Ray Desilvester, Mechanical Engineer
SIPS TEAM
David Hancock, SIPS Lead
Vijay Suchdeo, HDF Software Development and Data Processing
Andy Griffen, HDF Data Production

March 30, 2016
Document Version 1.1

SIMPL Greenland 2015 Campaign

Release 5 Data Product Documentation and Instrument Description

Table of Contents

March 30, 2016
Document Version 1.1

Release 5 Product Improvements and Limitations: 1 of 3

For details see Harding et al., SIMPL_2015_Rel5_Calibration_v1.1

Improvements over Prior Releases

Geolocation

- Precise pointing and timing biases determined from roll and pitch maneuvers over water have been applied during geolocation. Pointing angles for each channel with respect to the Applanix POS/AV 610 device used to measure position and attitude are given in /flight_parameters/angle_1064_mrad and angle_532_mrad. Timing biases, in seconds, for each channel between SIMPL and the Applanix are given in /flight_parameters/ tod_bias_1064 and tod_bias_532. The pointing angles and timing biases are constant values used for all processing.
- Time offsets for the NIR perpendicular, NIR parallel and Green perpendicular channels relative to the Green parallel channels are also applied during geolocation. These are determined for each granule individually based on along-beam surface slope correlation. They are reported in the /Auxiliary/Time Of Day Offset folders.
- After geolocation the elevation residual errors for flat surfaces (water departure from a flat surface during the maneuvers) are ~ 1 cm per 1° off nadir for each of the 16 channels. This corresponds to a horizontal error of ~ 10 cm per 1° off nadir.
- Absolute range biases for each of the 16 channels have also been applied during geolocation. They are reported in /flight_parameters/path_length_1064_mm and path_length_532_mm. They were determined based on ranging over a horizontal path to a fixed target at known distance. They are constant values used for all processing. Based on initial analysis these yield between-channel elevation accuracies at the decimeter level. Confirmation of the absolute accuracy with respect to an independent elevation source is pending.

Impulse Response Parameters

- Parameters in /Auxiliary/Impulse Response documenting the Transmit Echo Pulse (TEP) have been improved. The main and after pulse positions and widths are now computed using fits to the pulse leading and trailing edges improving their precision. The accuracy of the probability of detection parameter has also been improved.
- Parameters to characterize the TEP variability during a flight have been added in the MAIN PULSE TO MEAN OFFSET and CENTROID LINEAR FIT PARAMETERS folders in /Auxiliary/Impulse Response.

Release 5 Product Improvements and Limitations: 2 of 3

For details see Harding et al., SIMPL_2015_Rel5_Calibration_v1.1

Limitations

Snow, ice and water penetration depth

- The decimeter-level absolute elevation accuracies do not meet the objective of between-channel elevation accuracies at the centimeter level for the four channels on each beam. Work is ongoing to improve this accuracy. Improved absolute elevation biases will be reported on this web site when they become available.
- The Transmit Echo Pulse (TEP) method to monitor time variability of the elevation biases has not been implemented due to complexities in those measurements. Work is on-going to assess time-variability using the TEP products which are provided in /Auxilliary/Impulse Response. Results of that analysis will be reported on this web site when they become available.
- Calibration of the first photon bias for each of the 16 channels at the centimeter level, relating centroid elevation offset to probability of detection, is on-going. Calibration parameters will be reported on this web site when they become available.

Release 5 Product Improvements and Limitations: 2 of 3

For details see Harding et al., SIMPL_2015_Rel5_Calibration_v1.1

Limitations

Impulse Response Pulse Shapes

- The objective to provide time-varying pulse shapes for each channel not been reached in Release 5. The pulse shapes are provided in /Auxilliary/Impulse Histograms but due to complexities in the Transmit Echo Pulse (TEP) measurement method these are not reliable. Work is on-going to provide robust impulse responses which will be provided on this web site when they become available.

Signal Amplitudes

- The amplitude parameters in /Auxillary/PRN and channel ratios in /Auxillary/PRNR are based on un-calibrated photon counts and are therefore not consistent between channels and beams because of instrumentation effects. Channel scale factors to derive normalized amplitudes and ratios are provided in /Auxillary/ Ampitiude_Scale_Factors. These are currenlty set to 1. Work is on-going to determine these values which will be provided on this web site when they become available.

Missing Granules

- Some granules are missing, introducing data gaps, due to time of day errors in the granule start and/or end times. For some granules the time errors have been corrected and the data is on-line. Work is on-going to correct some of the other granules which will be posted as they become available. If you are missing critical data please let us know. Granules for July 21 cannot be corrected and will not be posted. It has not been determined if granules for July 23 and August 11 can be corrected.

Release 5 Product Improvements and Limitations: 2 of 3

Limitations

SIMPL Data delta_time Offset

- delta_times in the /Auxillary/PRN and /Auxillary/PRNR folders use a different reference time than the delta_times in the /impulse, /ins and /photon folders and so can not be used directly to align these data types. To align these data to GPS Time (seconds since the first GPS epoch) use:
  PRN and PRNR folders =
  delta_time + [604,800 sec/week x start_gpsweek (in /ancillary_data)] + [86,400 sec/day x day of week]
  Impulse, ins and photon folders =
  delta_time + gps_sec_offset (in /ancillary_data)
  Day of week for each flight is provided in Table 1.

Frame Camera Time Offset

- The frame camera file names provide hr:min:sec synched to GPS 1 pulse per second signals. For the July flights a -4 hour offset was applied to the file names during image recording converting to EDT. For the August flights the offset was set to 0.

Flight Date	GPS Week	Day of Week	Frame camera delta to offset to GPS time (hrs)
20150721	830	2	4
20150723	830	4	4
20150729	ASD calibration; no SIMPL data		4
20150730	831	5	4
20150803	832	1	0
20150804	832	2	0
20150807	832	5	0
20150810	833	1	0
20150811	833	2	0
20150812	833	3	0
20150813	833	4	0
20150814	833	5	0
20150817	834	1	0

SIMPL Greenland 2015 Campaign

Release 5 Data Product Documentation and Instrument Description

Campaign Overview

March 30, 2016
Document Version 1.1

SIMPL 2015 Greenland Campaign Team

From left to right

Goddard SIMPL Team:

Anthony Yu, Susan Valett, Philip Dabney, David Harding, Beth Timmons and Kurt Rush

Ames Applanix Installation and Processing:

Dennis Gearhart, James Jacobson

Goddard ICESat-2 Project Science Office:

Kelly Brunt, Kaitlin Walsh

Goddard ASD Profiling Spectrometer (not shown):

Chris Crawford

NASA Langley Aircraft Operations (not shown):

Rick Yasky, Mike Wusk, Andy Haynes, Dave Perez, Sean DeRubba

ICESat-2 Mission Overview

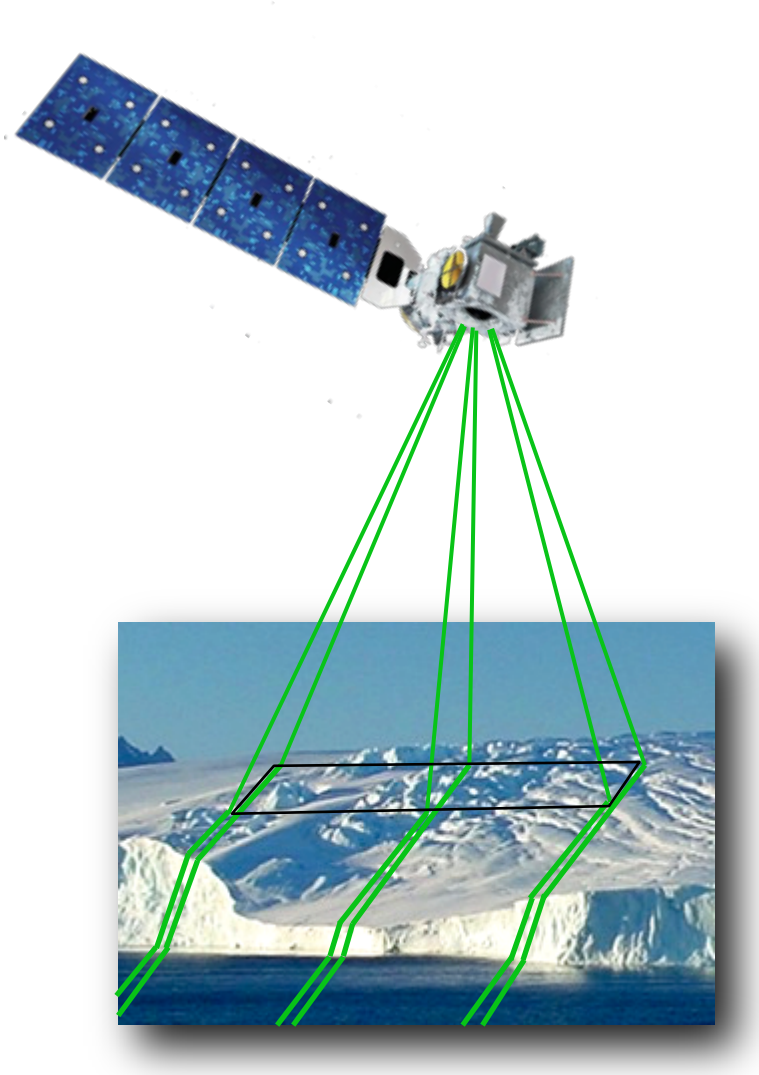

- Continuing polar warming is increasing the amount of melting during the summer contributing to ice sheet mass loss, resulting in sea level rise, and sea ice thinning
- ICESat-2 will measure changes in ice sheet elevation and sea ice thickness using the ATLAS laser altimeter
- ATLAS measures the round-trip travel time of high-repetition rate laser pulses along six beams (3 groups of 2) by measuring the pulse transmit time and return time of single photons (micropulse photon counting)
- Combining ranging distance, from travel-time, with beam pointing and spacecraft position determines the elevation of the surface along the beam profiles
- Repeating the measurements quantifies the rates of change in elevation and thickness
- The ATLAS laser operates at 532 nm (green wavelength)
- Penetration of the green laser pulses into ice, snow and water will cause the range to be biased too long introducing errors in the surface elevation profiles
- The bias magnitudes are sensitive to seasonal and annual changes in the surface physical properties

Slope Imaging Multi-polarization Photon-counting Lidar

- The airborne four-beam Slope Imaging Multi-polarization Photon-counting Lidar (SIMPL) is ideally suited to quantify green laser pulse penetration depths into snow, ice and water by operating at green and near infrared wavelengths
- It also definitively identifies the presence and, where shallow, the depth of melt ponds and the location of ice-free sea ice leads
- Nine science flights during July and August, 2015 in northwest Greenland, totaling 37 hours, collected data for a wide range of surface types
  - Interior dry snow, coastal ice surfaces with numerous melt ponds, melting sea ice and open ocean
- Concurrent hyperspectral AVIRIS data was collected to estimate snow and ice crystal size, particulate contamination and water content
  - To asses if they control the depth of green light penetration measured by SIMPL
- For campaign flight documentation see Brunt, K., T. Neumann and T. Markus, SIMPL/AVIRIS-NG Greenland 2015 Flight Report, NASA/TM–2015-217544, Oct. 2015.
  http://icesat.gsfc.nasa.gov/icesat2/data/simpl/docs/TM2015-217544.Brunt.pdf
- For SIMPL calibration documentation see Harding et al., SIMPL_2015_Rel5_Calibration_v1.1 available at the same web site.

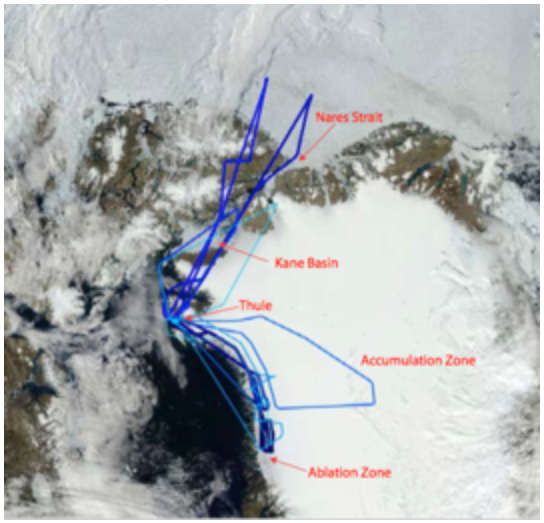

SIMPL's Measurements Characterize Surface Properties

Four beams

with surface properties from

8 amplitudes per beam

4 laser "hot spot" retro-reflectance

and 4 solar bi-directional reflectance

No laser NIR penetration so measures surface elevation:

| | 1064 nm parallel

_|_ 1064 nm perpendicular

Some laser green penetration into snow, ice and water so measures elevation that is biased low, dependent on the amount and depth of multiple scattering:

| | 532 nm parallel

_|_ 532 nm perpendicular

- The transmitter is an 11 kHz, 1064 nm micropulse laser with 1 nsec wide (FWHM), plane-polarized pulses
- A portion of the energy is frequency doubled to 532 nm
- The single laser beam is divided into four beams with co-aligned 1064 and 532 nm pulse energy
- The receiver separates the return energy into the two colors and into polarizations that are parallel || and perpendicular _|_ to the transmit plane
- Increasing _|_ photons are caused by increasing surface and volume multiple scattering
- 16 single photon counting modules (SPCM) and event timer electronics are used to time-tag the detection of individual photons with 0.1 nsec (1.5 cm) resolution
- The four photon "point cloud" profiles quantify elevation, roughness and slope with very high precision
- The number of detected laser-transmitted photons measures the surface "hot spot" retro-reflectance intensity at 0° phase angle
- The number of detected solar background photons measures the surface bi-directional reflectance in the same viewing geometry as the retro-reflectance
- Traditional laser altimeters only record one amplitude; laser retro-reflectance at one wavelength

SIMPL 2015 Beam Geometry and Channel Assignments

nadir view of beam positions: note that the positions are not the same as 2011 SIMPL data

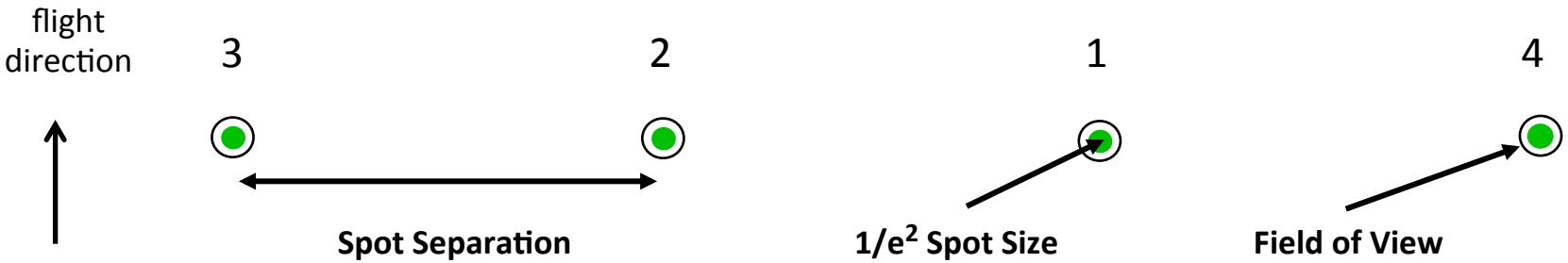

	Spot Separation	1/e^2 Spot Size	Field of View
Divergence:	2.35 mrad	130 urad	233 urad
At 2 km range:	4.7 m	0.26 m	0.45 m
At 3 km range:	7.05 m	0.39 m	0.0.67 m

Channel	Mode	Extension
9	1064 _|_	_A_3
10	1064 ||	_B_3
11	532 _|_	_C_3
12	532 ||	_D_3

Channel	Mode	Extension
5	1064 _|_	_A_2
6	1064 ||	_B_2
7	532 _|_	_C_2
8	532 ||	_D_2

Channel	Mode	Extension
1	1064 _|_	_A_1
2	1064 ||	_B_1
3	532 _|_	_C_1
4	532 ||	_D_1

Channel	Mode	Extension
13	1064 _|_	_A_4
14	1064 ||	_B_4
15	532 _|_	_C_4
16	532 ||	_D_4

Polarization state relative to the plane-polarized transmit beam: _|_ = perpendicular || = parallel

- SIMPL flight altitudes, above ground, typically varied between 2 to 3 km (6,500 to 9,500 ft)
- During the Greenland flights on July 30 (DOY 211), August 3 (DOY215) and August 4 (DOY 216) Channel 7 had an extremely weak signal due to a broken fiber. That was repaired for the subsequent flights.
- The beam divergence is 130 urad based on laboratory beam profile measurements of the micropulse laser used in 2009-2011. The new micropulse laser installed for 2015 may not have exactly the same beam divergence.
- The positions of the beam numbers have changed compared to 2009-2011 when it was 4, 3, 2, 1 from left to right

SIMPL 2015 Impulse Response Pulse Shapes

Horizontal path ranging calibration to flat target, Thule Air Force Base hanger, July 31, 2015

The impulse response is the convolution of the laser transmitter pulse shape and receiver pulse broadening

A laser after pulse is located 1.5 m following the main pulse. Its amplitude is strongest relative to the main pulse in the NIR perpendicular channels and reduced by about 50% in the NIR parallel channels. Its amplitude in the 532 nm channels is significantly decreased by the process of frequency doubling.

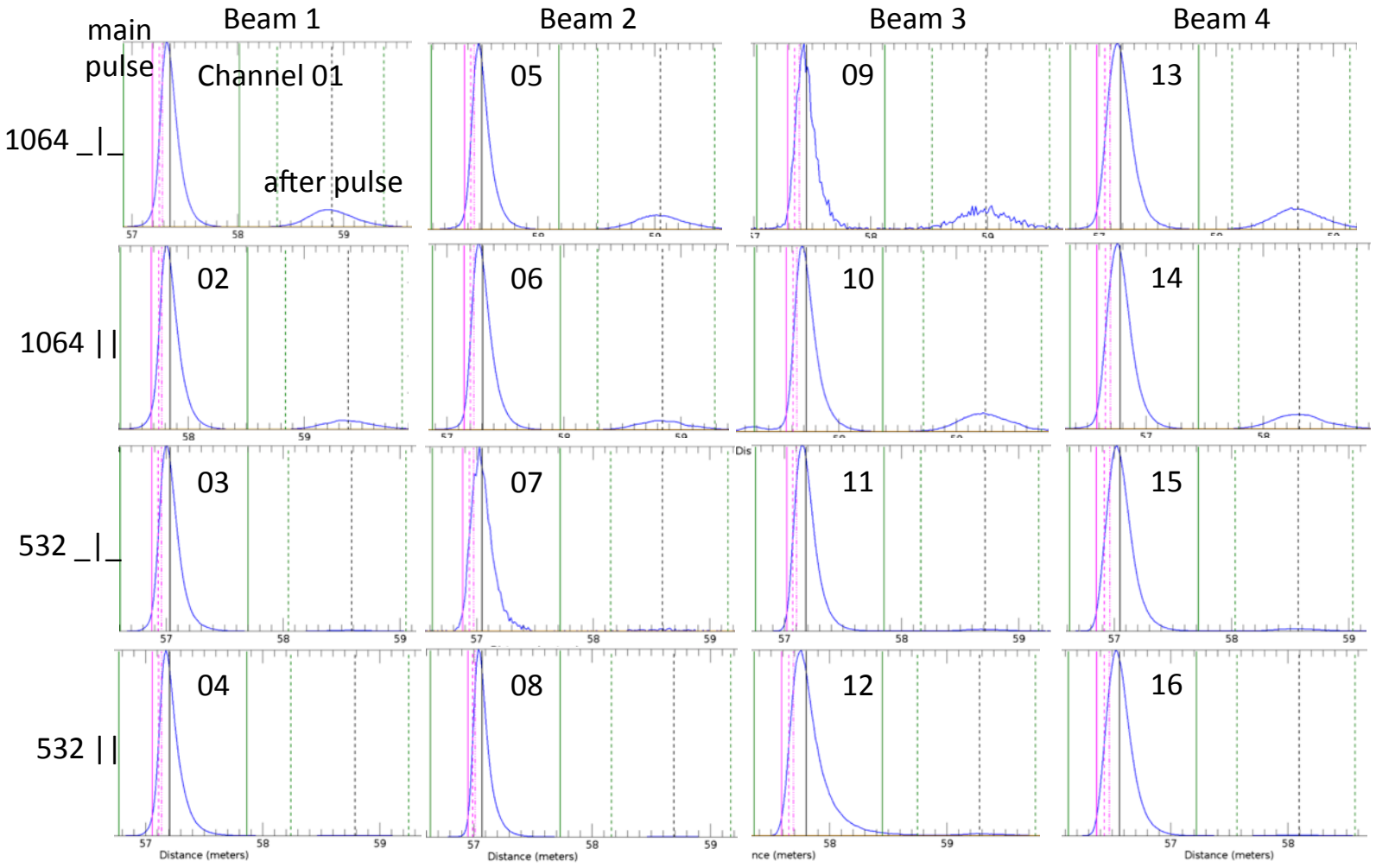

SIMPL Cryosphere Remote Sensing Capabilities (1 of 2)

SIMPL characteristics for snow and ice laser altimetry

- Co-incident Green 532 nm and near-infrared 1064 nm footprints enable direct comparison of the surface elevation from the NIR signal photons and depth of penetration from the green volume-scattered signal photons
- A narrow system impulse response (20 cm FWHM) and 0.1 nsec high precision timing (1.5 cm) achieves 8 cm range precision per photon and ~ 1 cm for 100 photons enable highly resolved penetration depth measurements.
- SIMPL uses small footprints (nominally 0.3 m diameter) to minimize within-footprint pulse broadening due to slope and roughness in order to isolate and quantify pulse broadening due to green penetration
- The small footprints with a typical photon density of 5 to 10 per meter per channel enables high resolution measurements of along-track surface elevation, slope, roughness, penetration and physical state

  (5 to 10% channel probability of photon detection per pulse) x (11,000 pulses per sec) / (110 m/sec ground speed)
- The total cross-track separation of the four beams is typically between 13 to 20 m, dependent on altitude, enabling assessment of the variability of the surface properties at the ICESat-2 ATLAS footprint scale
- The four beams enable measurement of cross-track surface slope and curvature at the ATLAS footprint scale
- The number of _|_ photons relative to || increases as surface and volume multiple scattering increases providing information on physical properties (e.g. snow grain size, reflectance and roughness)
- The number of green signal photons relative to NIR is sensitive to the physical state of the surface (e.g. snow, firn, ice, dirty ice) because of reflectance differences at these wavelengths
- The number of signal photons (laser “hot spot” retro-reflectance) relative to background noise photons (solar BRDF bi-directional reflectance) is sensitive to increasing slope (changing the solar BRDF incidence angle) and increasing roughness (increasing the solar shadow fraction).

SIMPL Cryosphere Remote Sensing Capabilities (2 of 2)

SIMPL signal characteristics for water surface, column and bottom laser altimetry

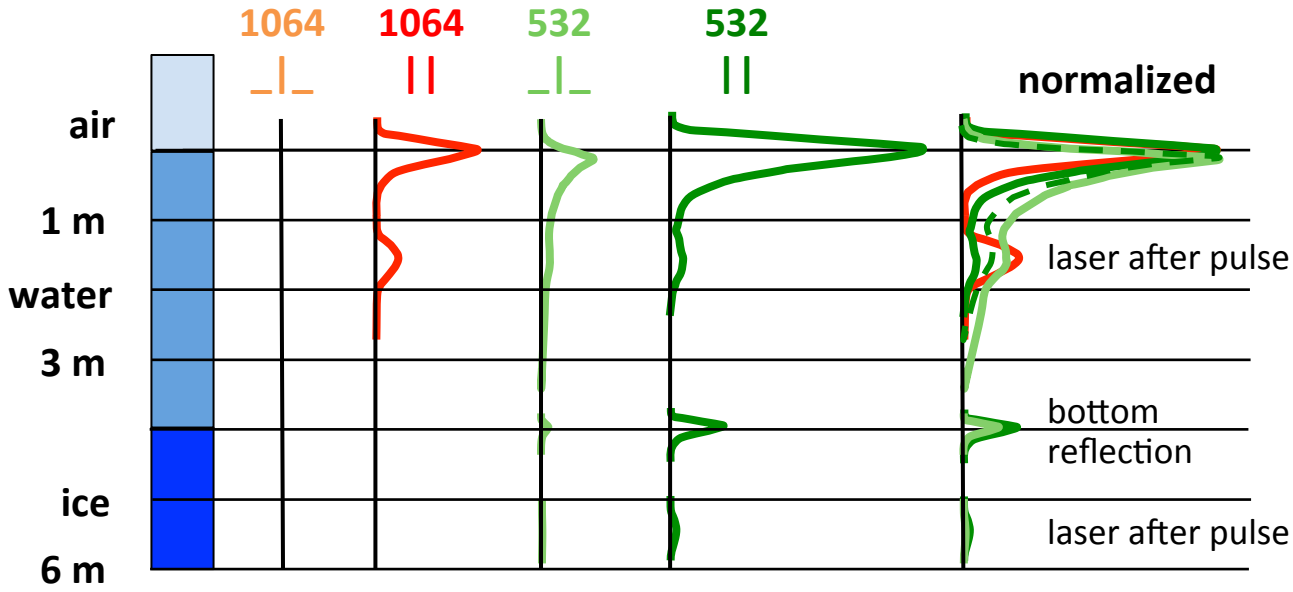

Nominal Case

- || photons are only returned from the surface because NIR light is absorbed in the sub-surface due to water's very high absorption coefficient.
- _|_ photons are absent because the water surface is specular thus only single scattering reflections occur and no photons are converted to _|_ state. A very weak signal is sometimes present which may be due incomplete separation of _|_ photons from the || signal.
- || photons are reflected from the surface and also the water column due to single scattering reflections from particulates. The column scattering component is indicated by the green dashed line. There may be bottom return if the water is sufficiently clear and shallow.
- _|_ photons are not reflected from the specular surface. An increasing fraction of the || photons in the water column are converted to _|_ as multiple scattering from particulates increases. Like || there may be a _|_ bottom signal. If the bottom is glassy specular ice there will be no signal.
- The depth of 532 nm scattering and the rate of || vs. _|_ extinction is a function of the water optical depth which is dependent on the particulate concentration.

Clear melt pond case

- Because melt pond water can be very clear with few particulates (depending on the contamination level in the source snow and ice) there often is minimal to no green water column scattering component.
- || will have a surface return and a bottom return if the water is sufficiently clear and shallow.
- _|_ will have no surface return and no bottom return because there will be no _|_ photons generated in the water column to reflect.

Off nadir incidence case

- The strength of the surface returns decrease with increasing beam incidence angle and decreasing wind-driven roughness. If the incidence angle is large enough and/or the surface is smooth enough || and || surface returns will not be detected because they are directed away for the receiver by the specular reflection. As above, green water column and bottom signals will depend on the water clarity and depth.

SIMPL Water Column Signal Example

2011 Gulf of Mexico 20 km Off-shore
Deep water so no bottom signal

Photon Point Cloud Profiles for One of Four Beams

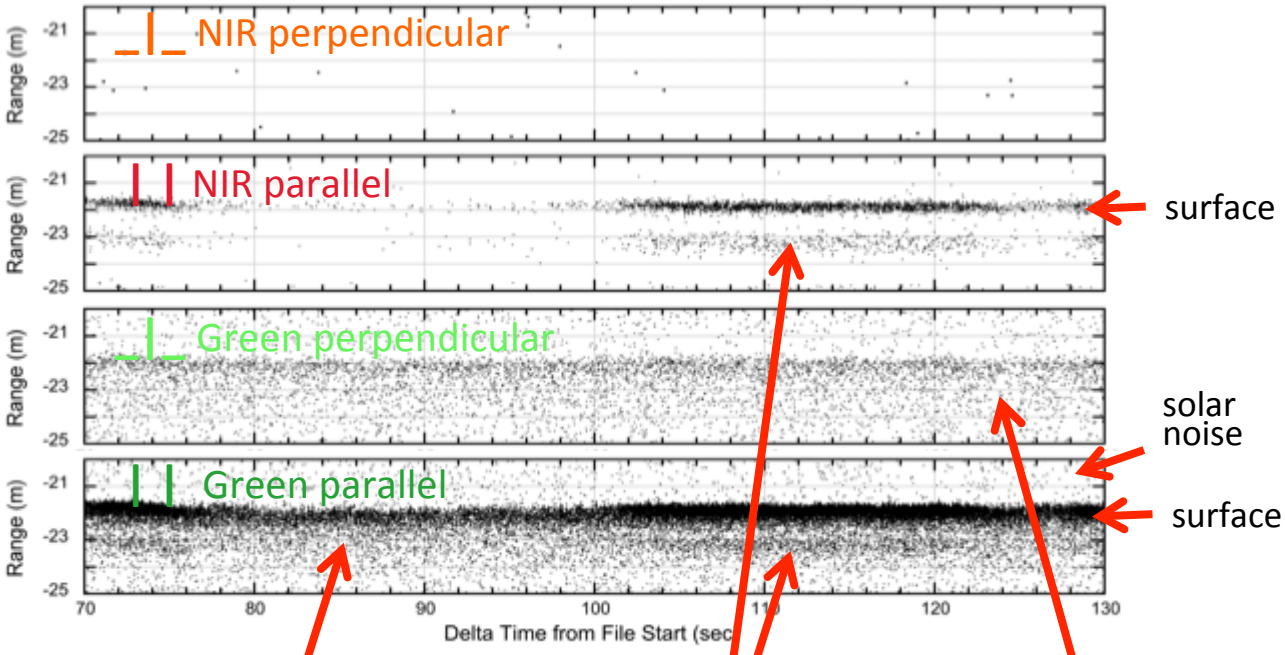

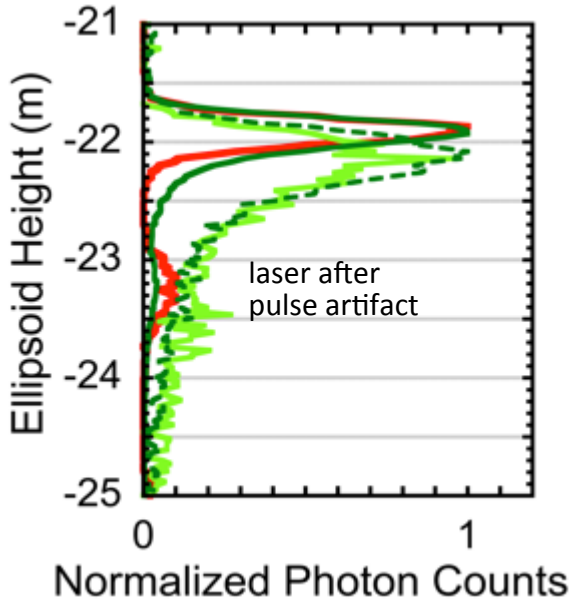

all sub-surface scattering no specular surface signal due to high incidence angle during aircraft turn

laser after pulse

all sub-surface scattering no _|_ surface return

dashed green line is sub-surface component of | | signal observed where there is no specular return

SIMPL Ice and Water Signal Example

2015 Nares Strait Pack Ice with Melt Pond Network

frame camera image

- Photon point clouds identify the location of melt ponds by the absence of 1064 and 532 perpendicular surface returns
- 532 nm penetration into ice and water is seen in the volume scattering below the surface where the photon density is higher than the background noise
- Low signal strength from the ice for 1064 _|_ is because NIR multiple scattering is rare
- Stronger 532 _|_ ice signal is because green multiple scattering is more frequent due to penetration and higher albedo
- The histogram shapes are broadened due to surface penetration, roughness and slope
  Surface slope is because aircraft roll effect is not removed in this range data

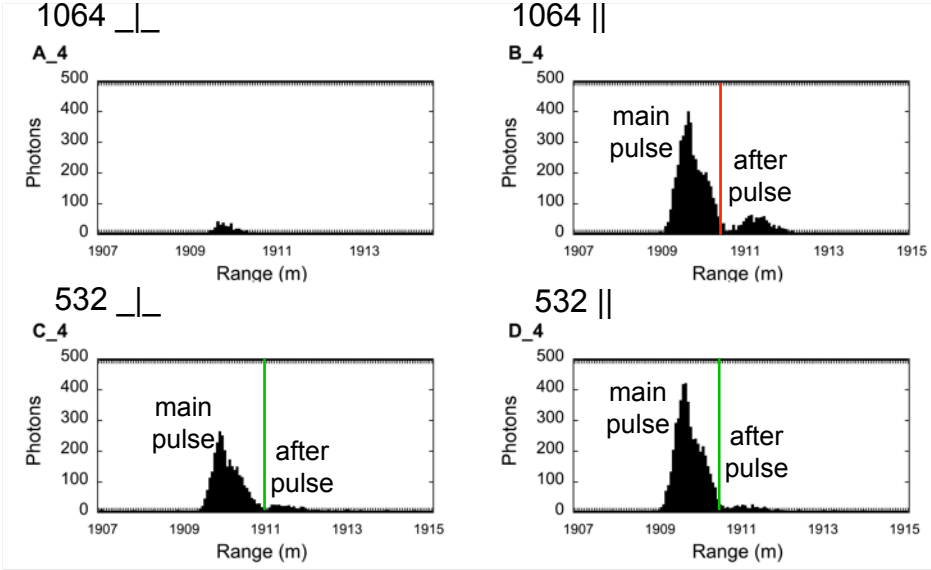

Photon range histograms for the 4 channels

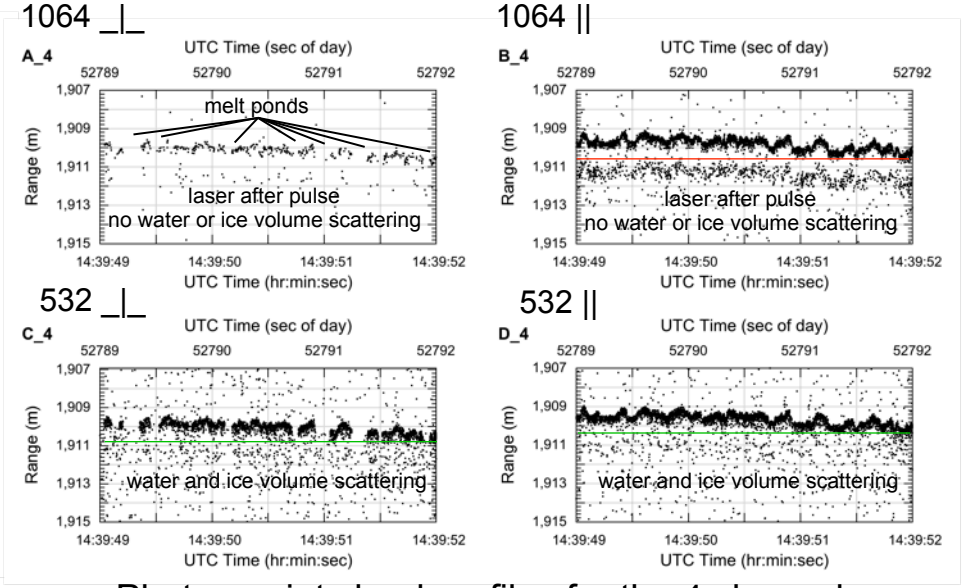

Photon point cloud profiles for the 4 channels

350 m long profile for Beam 4

Horizontal Path Range and Beam Geometry Testing at Goddard

Firing at Building 33 C Wing Rooftop Wall and Trees out G Wing Penthouse Door

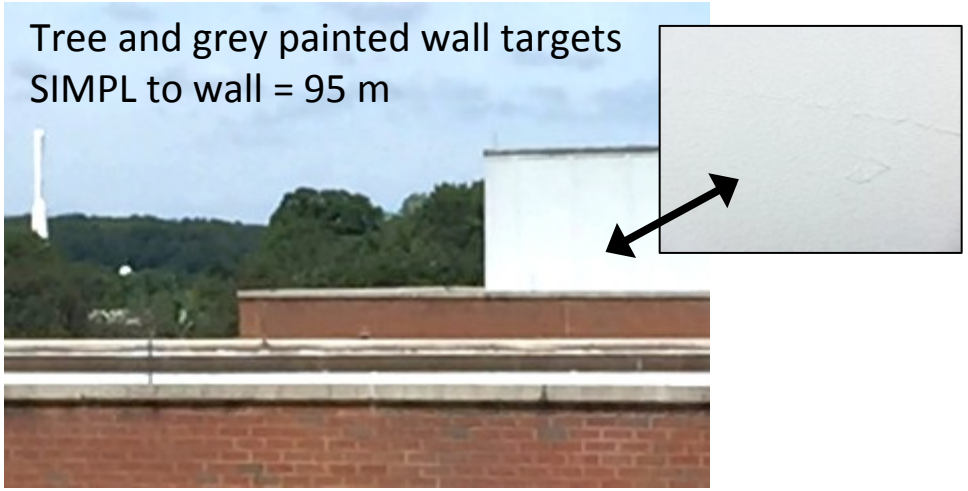

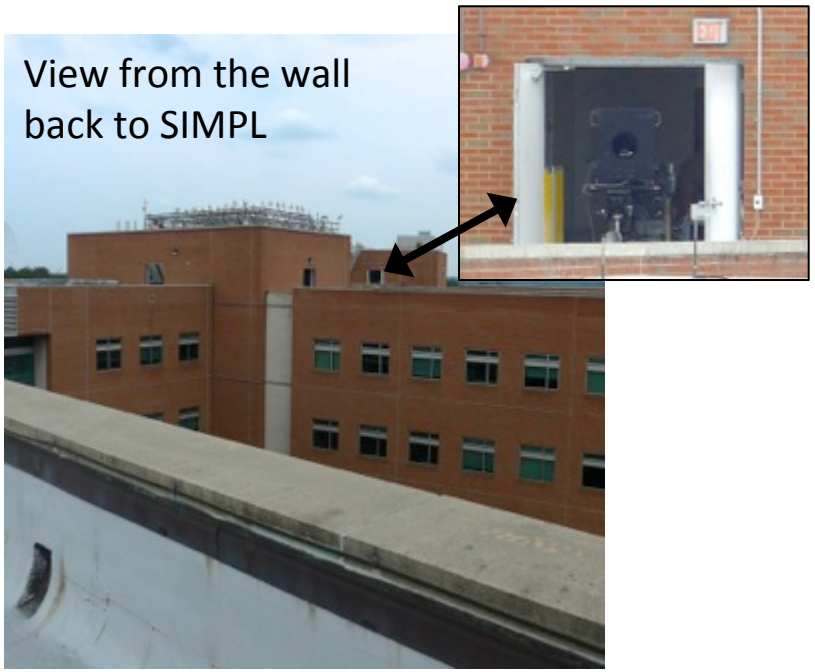

SIMPL oriented horizontally on a tripod and data handling electronics

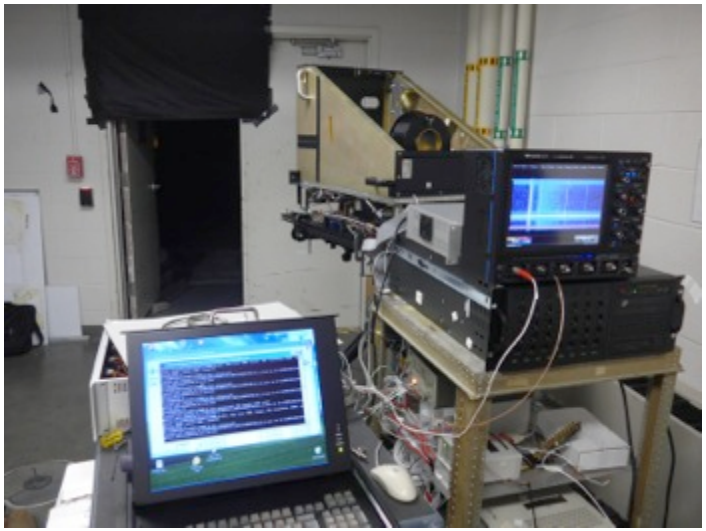

Horizontal Path Range and Beam Geometry Testing at Goddard

Firing at Building 33 C Wing Rooftop Wall and Trees out G Wing Penthouse Door

Horizontal Path Range and Beam Geometry Testing at Goddard

Nighttime View of Beams on the Building 33 C Wing Wall

- Beam 2 green laser spots at 95 m ranging distance
- Eight successive photos show laser scintillation
- 1/20 second exposure = 550 laser fires per photo

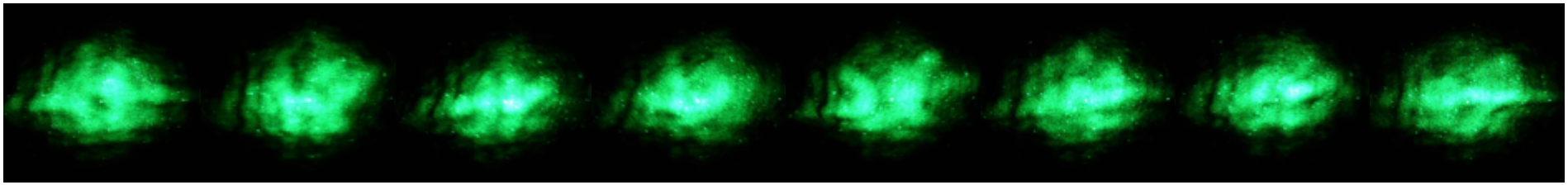

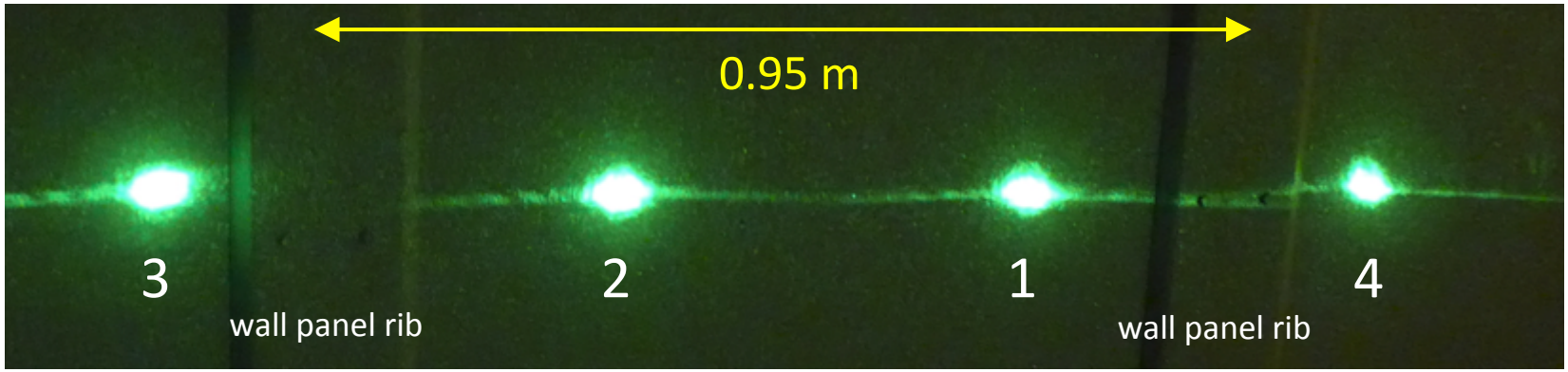

flight direction

Installation on NASA Langley N528NA King Air

Fork lifting 150 lb SIMPL transceiver into plane

SIMPL installed over optical port behind Command and Data Handling computer rack.

Electronics racks installed behind SIMPL. Each rack is ~160 lbs.

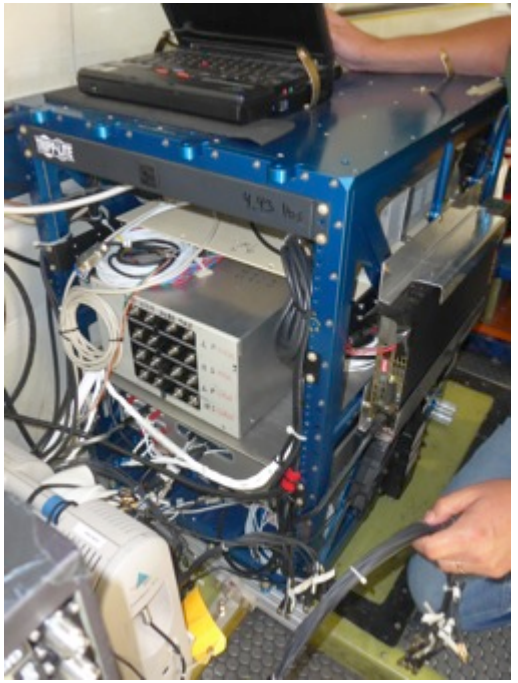

Measurement Objectives for 2015 SIMPL Campaign in Northwest Greenland

Campaign team and NASA Langley King Air at Thule

Open water green light penetration depth, ice freeboard and pack ice breakup

Green light penetration depth is a function of snow and ice grain size and contaminant concentration

Smooth ice sheet and outlet glacier topography

Ablation zone topography and melt water distribution and depth

SIMPL Greenland 2015 Campaign

Release 5 Data Product Documentation and Instrument Description

SIMPL HDF Data Products

March 30, 2016
Document Version 1.1

Top level h5 granule structure

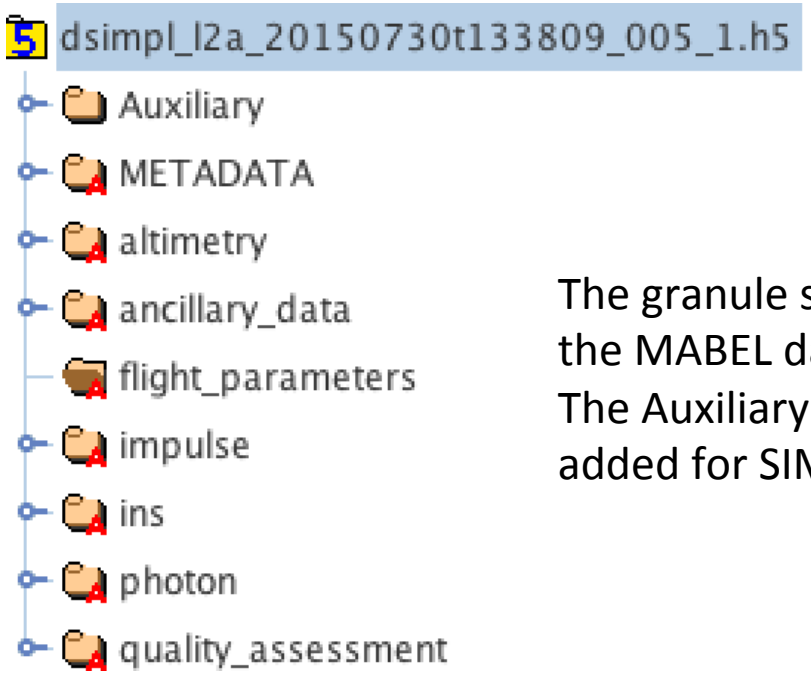

The granule structure is similar to that used for the MABEL data distribution.
The Auxiliary and impulse folders have been added for SIMPL-specific data products.

Photon Folder Contents

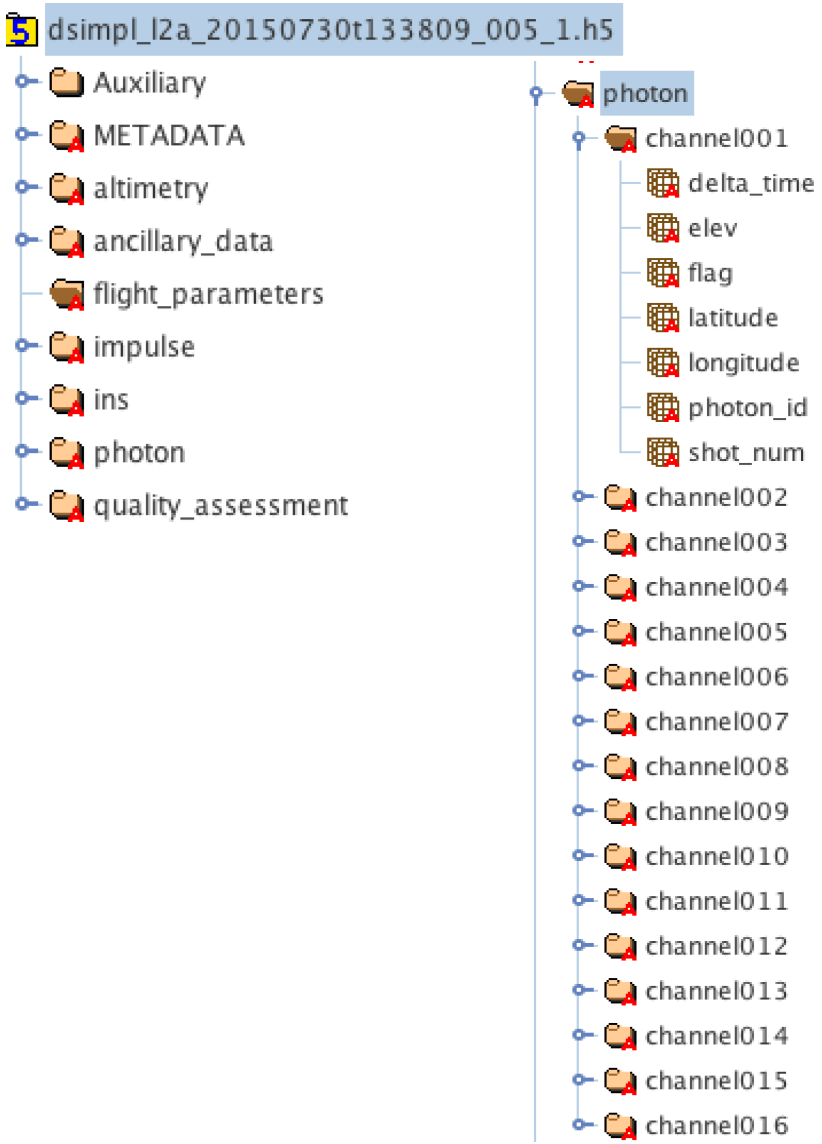

Standard geolocated photon point clouds for each of the 16 channels

Delta_time is the offset with respect to the GPS reference seconds given in /ancillary_data/gps_sec_offset.
GPS Time (seconds since the first GPS epoch) = delta_time + gps_sec_offset.

The height range of the photons is
Land and near-shore ocean: DEM +1,000 m to -500 m
Ocean: ±100 relative to MSS
Designation if the granule is treated as land or ocean, and the source for the DEM, is given in /altimetry/dem_drm/dem_flag

Elev, latitude and longitude are referenced to the WGS-84 reference ellipsoid, defined by two parameters:
Semi-major axis, a = 6378137 meters
Inverse flattening 1/f = 298.257223563

Photons in a range window from 200 m to 5 km below the aircraft (extending ~ 2 km past the surface) are available in an ICESat-2 project archive for atmosphere studies (this data is not on-line and is not geolocated)

Impulse Folder Contents

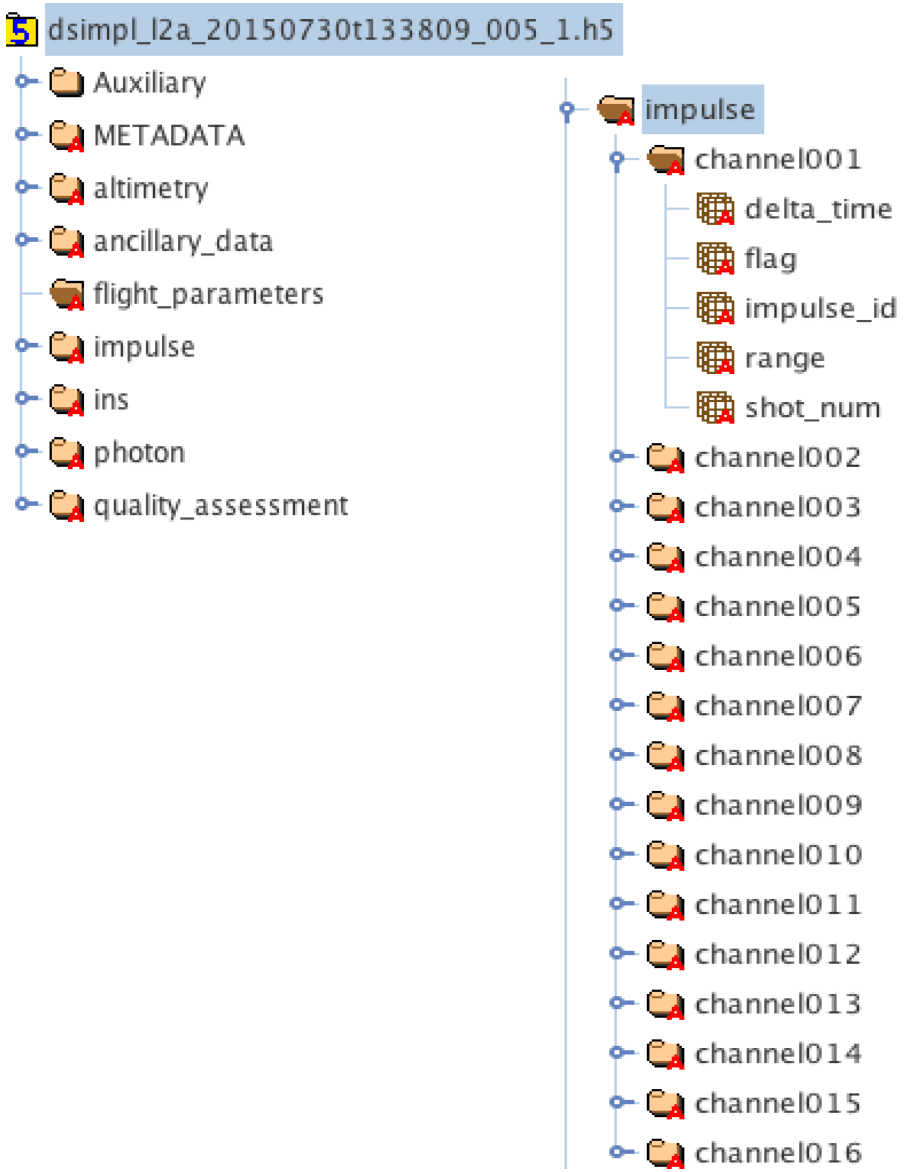

Transmitter Echo Pulse (TEP) impulse response photon point clouds for each of the 16 channels

Transmit pulse photons are delayed through a fiber spool and directed into the receiver to characterize the instrument impulse response pulse shapes and range biases. The range window extends from 25 to 45 m range with the impulse responses at ~ 35 m. These photons are not geolocated.

Delta_time is the offset with respect to the GPS reference seconds given in /ancillary_data/gps_sec_offset.
GPS Time (seconds since the first GPS epoch) = delta_time + gps_sec_offset.

Auxiliary Folder Contents

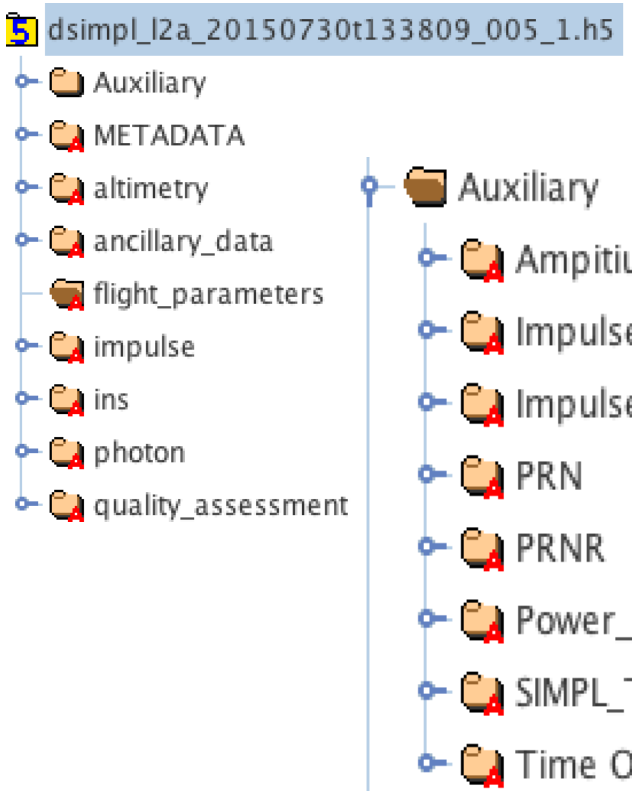

For normalizing signal strengths between channels*

Range histograms of the TEP impulse photons

Parameters describing the TEP impulse response

Along track signal and noise attributes

Along track ratios between signals and noise

Laser output power time series

Receiver filter block temperature time series

Time offsets between channels used in geolocation

*Scale factors in Release 5 are set to 1.

Correct factors will be provided when the amplitude calibration is completed.

TEP Impulse Histograms Folder Contents

- Auxiliary
  - Ampitiude_Scale_Factors
  - Impulse Histograms
    - Bin_Minimum
    - chan_001_Photon_Counts
    - chan_002_Photon_Counts
    - chan_003_Photon_Counts
    - chan_004_Photon_Counts
    - chan_005_Photon_Counts
    - chan_006_Photon_Counts
    - chan_007_Photon_Counts
    - chan_008_Photon_Counts
    - chan_009_Photon_Counts
    - chan_010_Photon_Counts
    - chan_011_Photon_Counts
    - chan_012_Photon_Counts
    - chan_013_Photon_Counts
    - chan_014_Photon_Counts
    - chan_015_Photon_Counts
    - chan_016_Photon_Counts

Starting range for each histogram bin from 25 to 45 m with 0.015 m sampling

Number of photon counts in each histogram bin

Example histogram showing the full range window (top), the segment from 33 to 38 m (bottom) which contains the impulse response and the range positions of parameters provided in the Impulse Response Folder

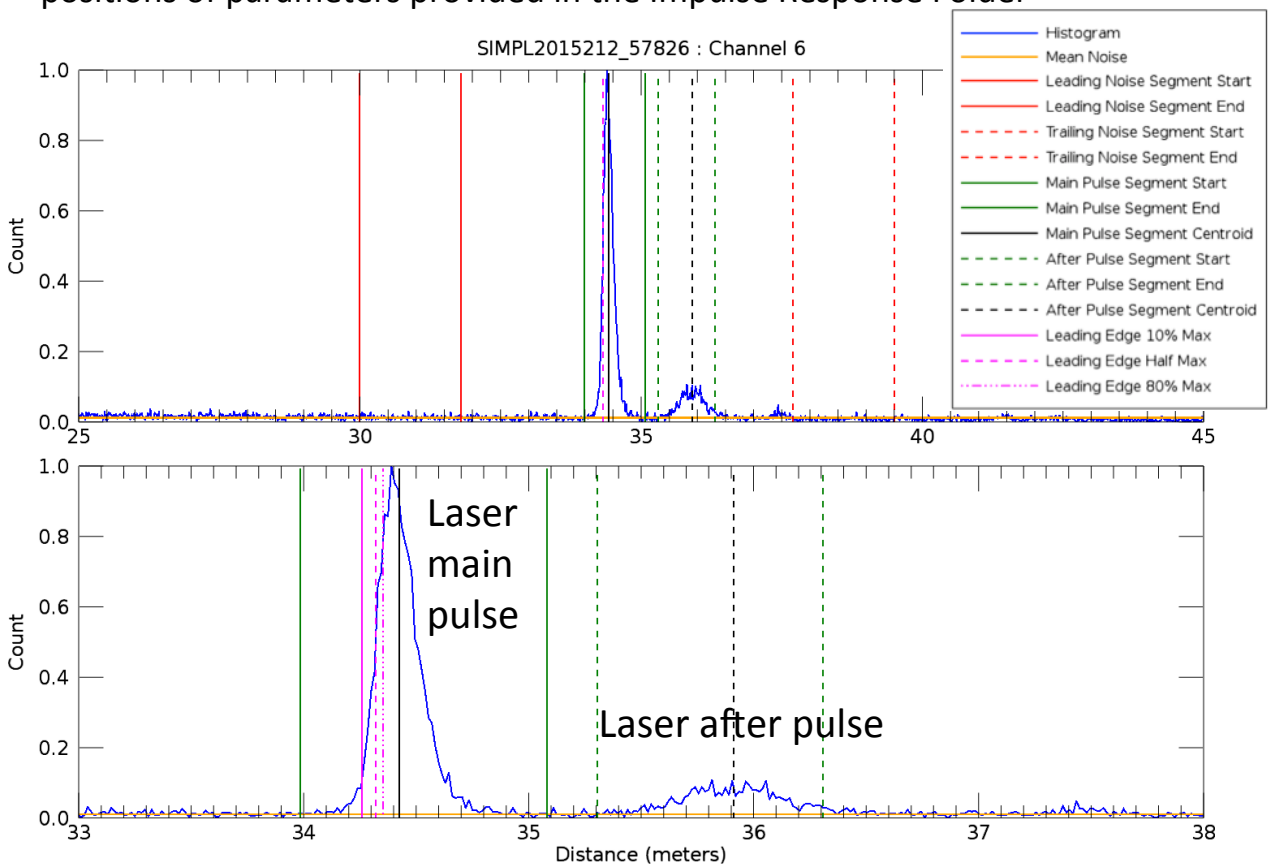

TEP Impulse Response Folder Contents

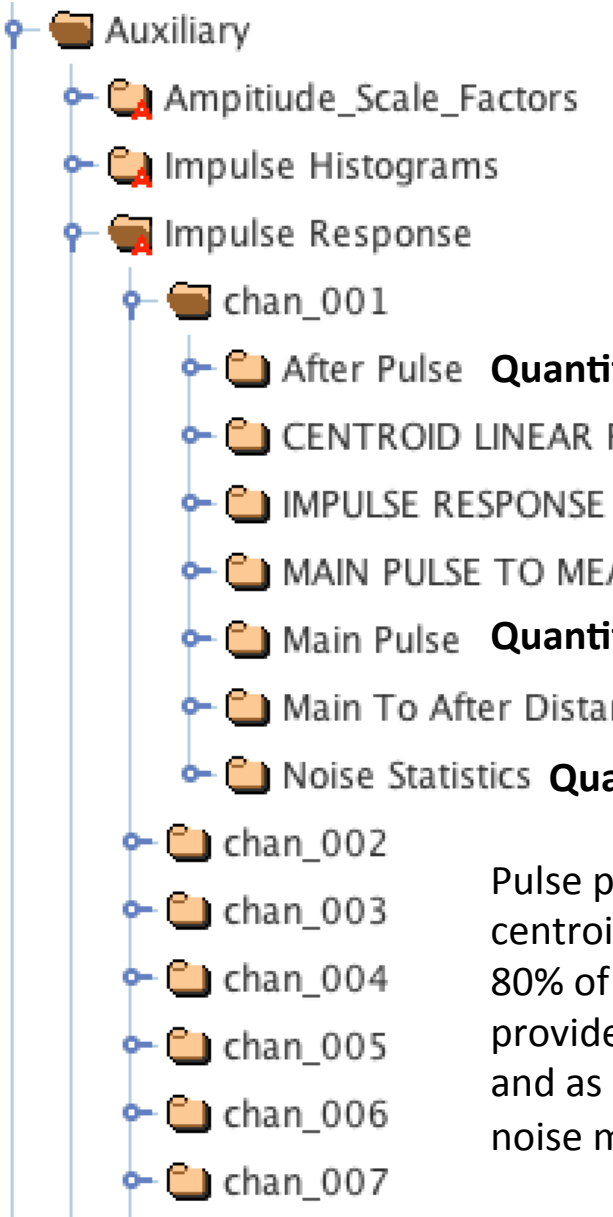

Quantify the position, shape and amplitude of the after pulse

See next slide

Input parameters used in the impulse response analysis

See next slide

Quantify the position, shape and amplitude of the main pulse

Quantify the separation of the main and after pulses

Quantify the background noise mean and standard deviation

Pulse positions and separations are provided for the mode (peak), centroid (mean), and leading edge thresholds at 10%, 50% (half max) and 80% of the mode amplitude. Pulse widths (leading to trailing edge) are provided for the three thresholds. Amplitudes are reported for the modes and as probabilities of detection (number of detected photons above the noise mean divided by the number of laser fires).

TEP Impulse Response Folder Contents

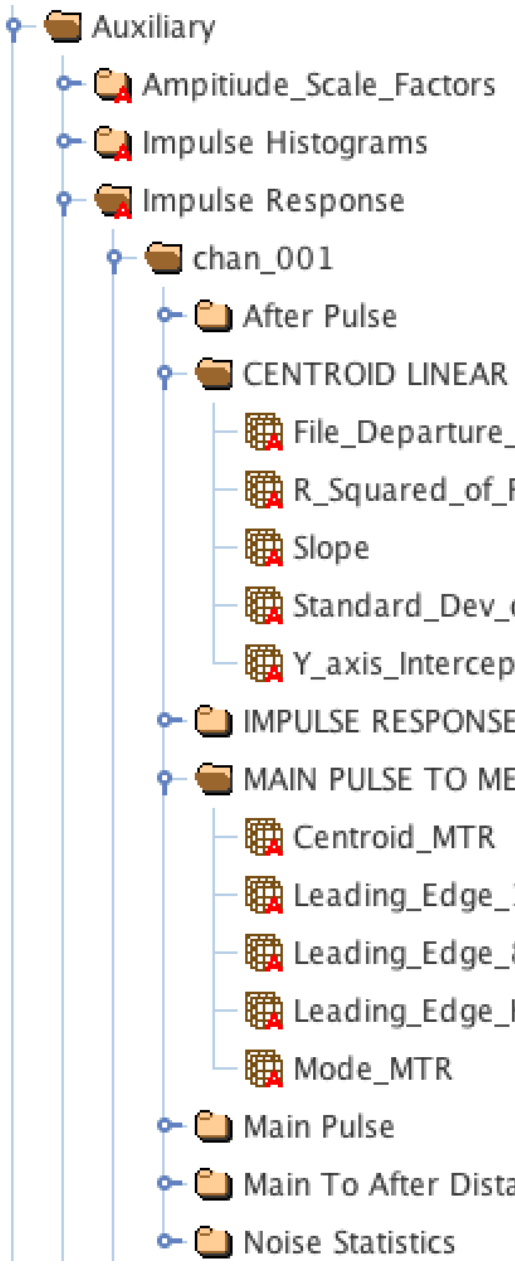

Parameters are provided that give an indication of the time variability of the main pulse position during the course of a flight.

Quantify a linear fit to the main pulse centroid position for all granules collected during a flight and give the departure from that fit (the delta between the granules centroid and the linear fit).

Quantify the main pulse offsets from the mean for all granules collected during a flight for each of the five position parameters.

TEP Impulse Response Folder Contents

Example of time series plots for two of the TEP impulse response parameters showing main pulse probability of detection and centroid range for each of the granules collected during the flight on August 12, 2015. Channels with very low probability of detection (03, 09, 15, 16) causing noisy results are plotted as very thin lines.

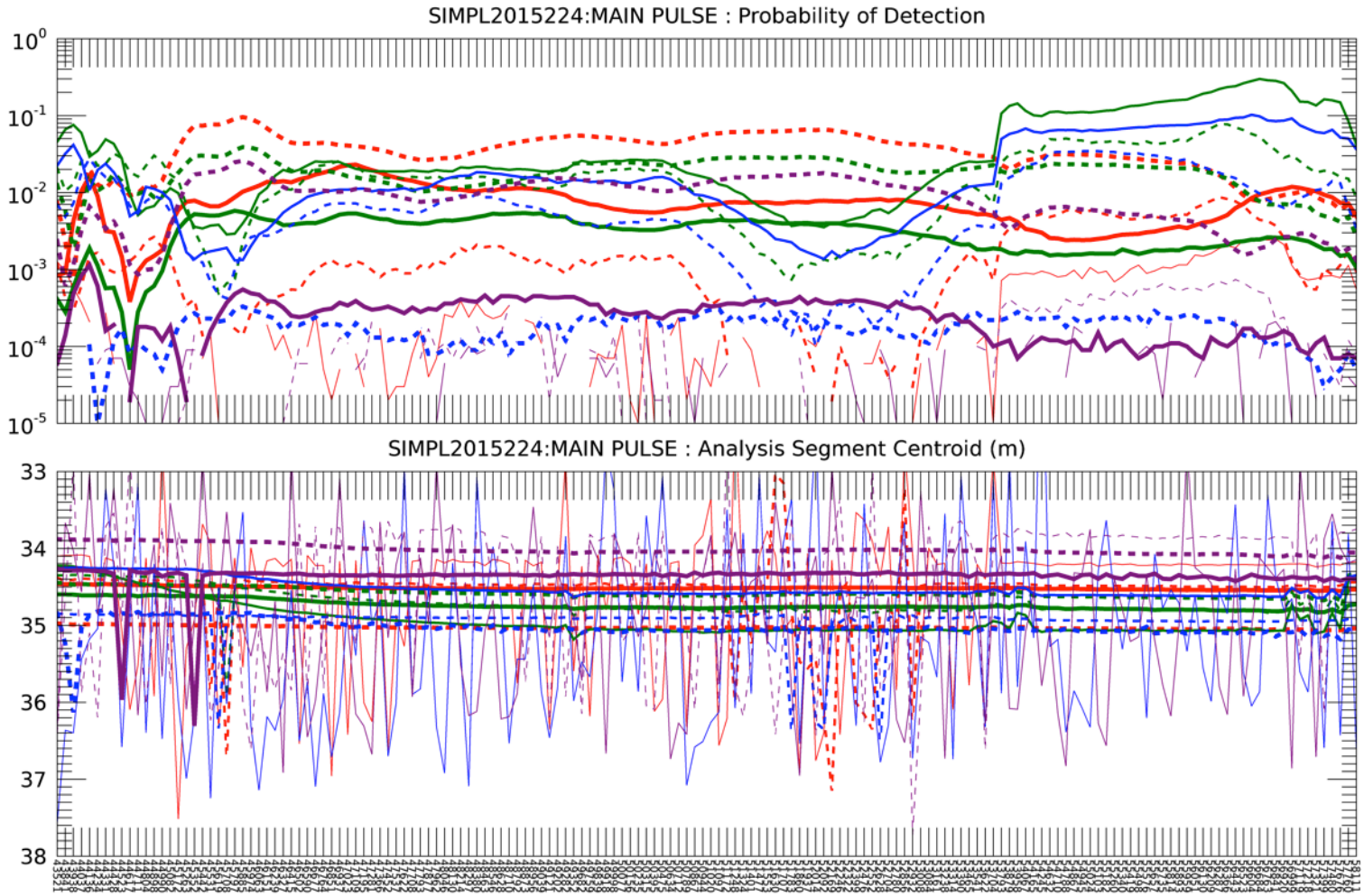

Channels

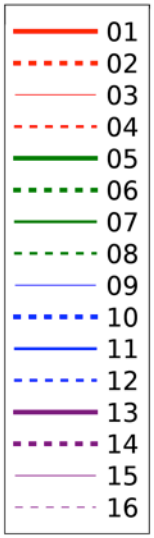

Color = beam
Thick = NIR
Thin = Green
Solid = _|_
Dashed = | |

TEP Impulse Response Folder Contents

Example of two plots for parameters associated with the linear fit to the TEP impulse response centroids. The top shows each granules departure from the linear fit. The bottom shows the R^2 of the fits. Channels with very low probability of detection (03, 09, 15, 16) causing noisy results are plotted as very thin lines.

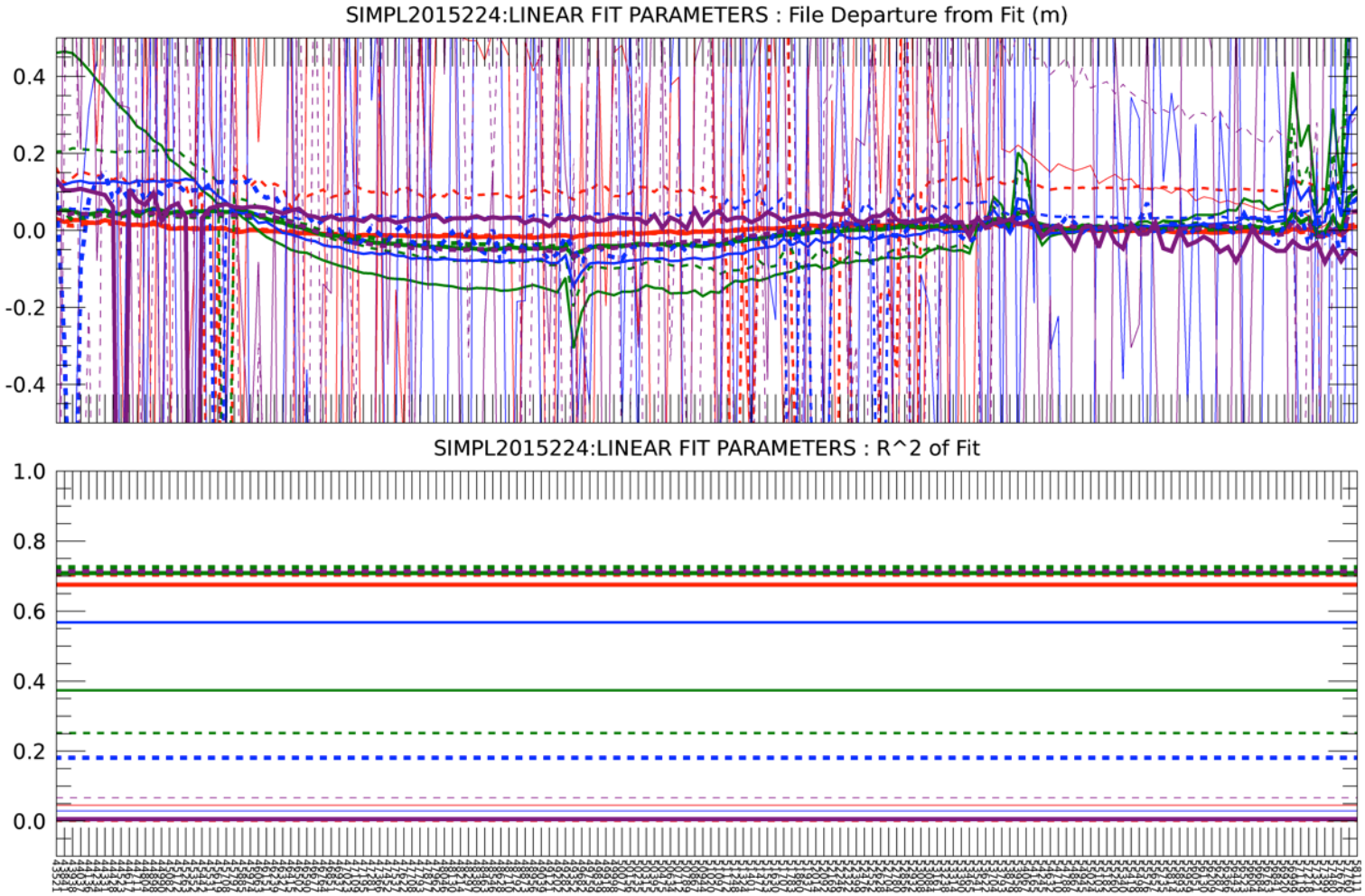

Channels

01
02
03
04
05
06
07
08
09
10
11
12
13
14
15
16

Color = beam
Thick = NIR
Thin = Green
Solid = _|_
Dashed = | |

PRN Folder Contents

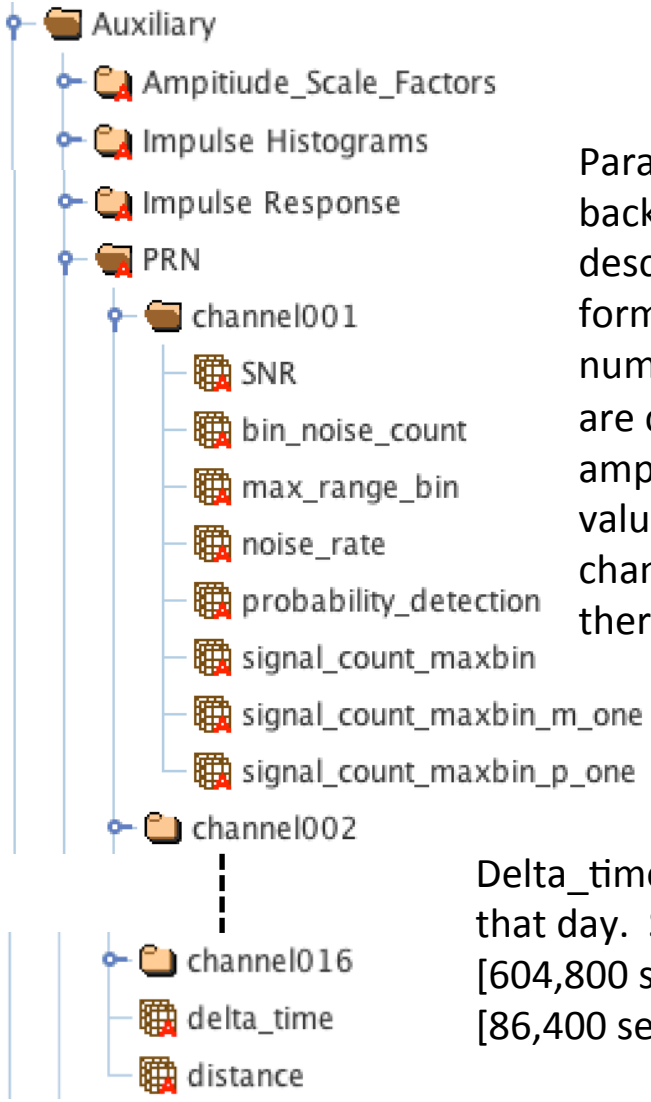

Parameters are provided at 10 Hz that quantify laser signal and solar background noise amplitudes along each beam profile using the method described on the following two slides. Note that the SNR is not a standard formulation. It is computed as the PD divided by the noise rate, not the number of signal photons divided by the number of noise photons. They are computed using the observed number of photons in a channel. The amplitudes have not been calibrated for instrumentation effects so the values are not comparable between channels. Scale factors for each channel will be provided so that instrument affects can be removed thereby normalizing the between channel signal and noise strengths.

Delta_time is the offset in seconds with respect to midnight of that day. Seconds since the first GPS epoch = delta_time + [604,800 sec/week x start_gpsweek (in /ancillary_data)] + [86,400 sec/day x day of week]

Distance is an approximate distance along the profile assuming a nominal aircraft ground speed of 105 m/sec.

PRN Statistics Computed Using a Basic Surface Tracking Algorithm

The probability of detection (PD) and signal-to-noise ratio (SNR) are based on surface signal photons

- The method does not classify each photon
  The surface is defined based on maximum photon density
- Surface is tracked using Channel 2 and then applied to all channels
  Channel 2 is NIR Parallel Beam 1 which usually has the highest SNR
- The "surface" is the bin with the maximum number of photons (max_range_bin)
- Bins are 0.1 seconds in duration (frame) by 15 m in range for snow, ice and water (2009 and 2015) and 45 m for non-arctic land to handle steep topography, buildings and/or tall vegetation (2010 and 2011 data)
  The frame length is ~ 11 m, dependent on ground speed (nominally 100 to 120 m/sec)
- Max_range_bin can be noise, a dense cloud top or the true surface. If it is noise the max_range_bin will randomly appear anywhere in the search window which extends from 200 m below the plane to the end of the acquisition window (13 km in 2009-2011) or to the end of a post-processing gated window (5 km in 2015).
- Surface tracking initiation begins at the start of a granule and determines when max_range_bin is continuous for 50 frames (~ 0. 5 km). Continuity is defined as the max range bin being within ± 3 bins of the max bin in the preceding frame for 15 m bins and ± 2 for 45 m bins
  Initiation can start on a cloud top if dense clouds occur at the start of the granule within the search window
- Once 50 continuous frames are identified then the tracking frame by frame proceeds starting with the max_bin mode for the 50 frames.
- The signal used to compute PD and SNR is the sum of photons in the max_range_bin and the bins that are 1 above and 1 below max_range_bin in the same frame, with the solar background noise photons per bin in that frame subtracted from each
  Noise photons per bin is the average of a 30 bin window that stops 100 bins from the end of the data window
  The noise rate is the number of noise photons per second in units of mHz.
  The PD is the number of signal photons, in both the main and after pulses, divided by the number of laser fires in 0.1 sec assuming a nominal laser fire rate of 11.4 kHz.
  The PD and noise rate are computed at 10 Hz then smoothed using a running 5 bin averaging window.
  The SNR is a non-standard computation equal to the PD divided by the noise rate. It is not the number of signal photons divided by the number of noise photons.

Algorithm Method when Surface Tracking is Lost

Tracking is reset when max_range_bin surface continuity fails

- Surface tracking can fail (max_range_bin change exceeds the ± 3 or ± 2 bin limit)
  - pointing at large angles over specular smooth water or ice (turns; roll & pitch)
  - ranging through clouds
  - surface very abruptly changes elevation
  - aircraft very abruptly maneuvers (roll and/or altitude; unlikely)
- Where surface continuity is lost the last max_range_bin is projected at a constant range for 8 frames (~90 m), testing for continuity at each frame
- If continuity fails for the 8 frames the tracking initiation is restarted
- The reset can cause the "surface" to jump from the true surface to a dense cloud top or from a cloud top to the true surface
- All PRN and PRNR results are invalid for frames where max_range_bin is not the true surface
- There is no flag on the product to identify frames that are not the true surface
  It is difficult to be certain given the variety of max_range_bin patterns that can occur
- Examination of max_range_bin profiles can provide insight into when the true surface is lost as can outliers in the probability_detection, noise_rate and SNR values
  Threshold edits could be applied to any of these values to exclude non-surface frames

Greenland Ablation Zone Probability of Detection Example from PRN Folder

Sampled at 10 Hz (~ 11 m); Smoothed with running 5 bin average (~55 m)

August 12, 2015
Ablation Zone
~ 7,500 ft AGL
55° doubler temp
1.3 min granule
15:07:20

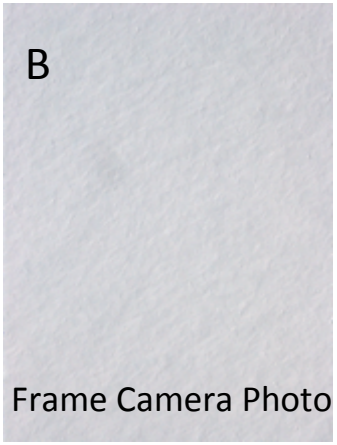

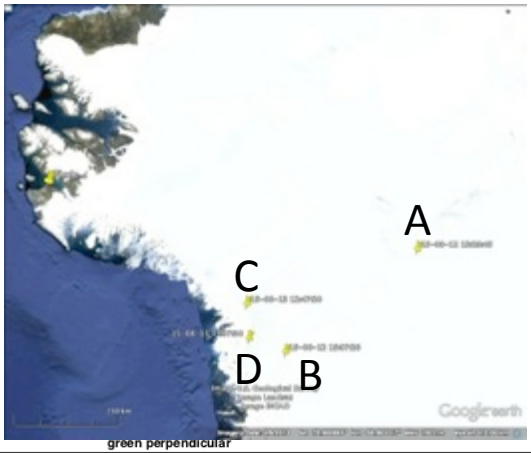

Items of Note:

- Uniform PD's over uniform surface
- Source of green spikes not known
- Green _|_ ~ equal to || due to significant multiple scattering
  - bright & penetration
- NIR _|_ low compared to || due to minimal multiple scattering
  - darker & no penetration

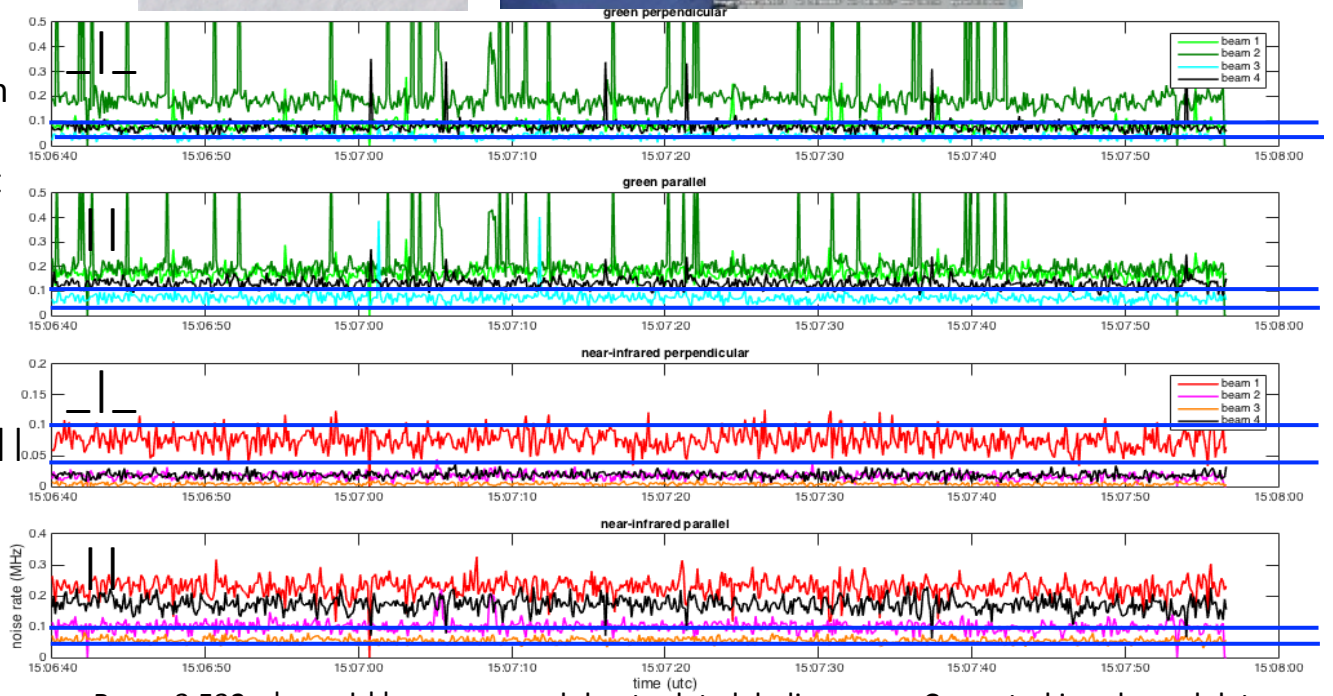

PD Goal
10%
4%

Beam 3 532 _|_ and || are swapped due to data labeling error. Corrected in released data.

Greenland Ablation Zone Probability of Detection and Noise Rate from PRN Folder

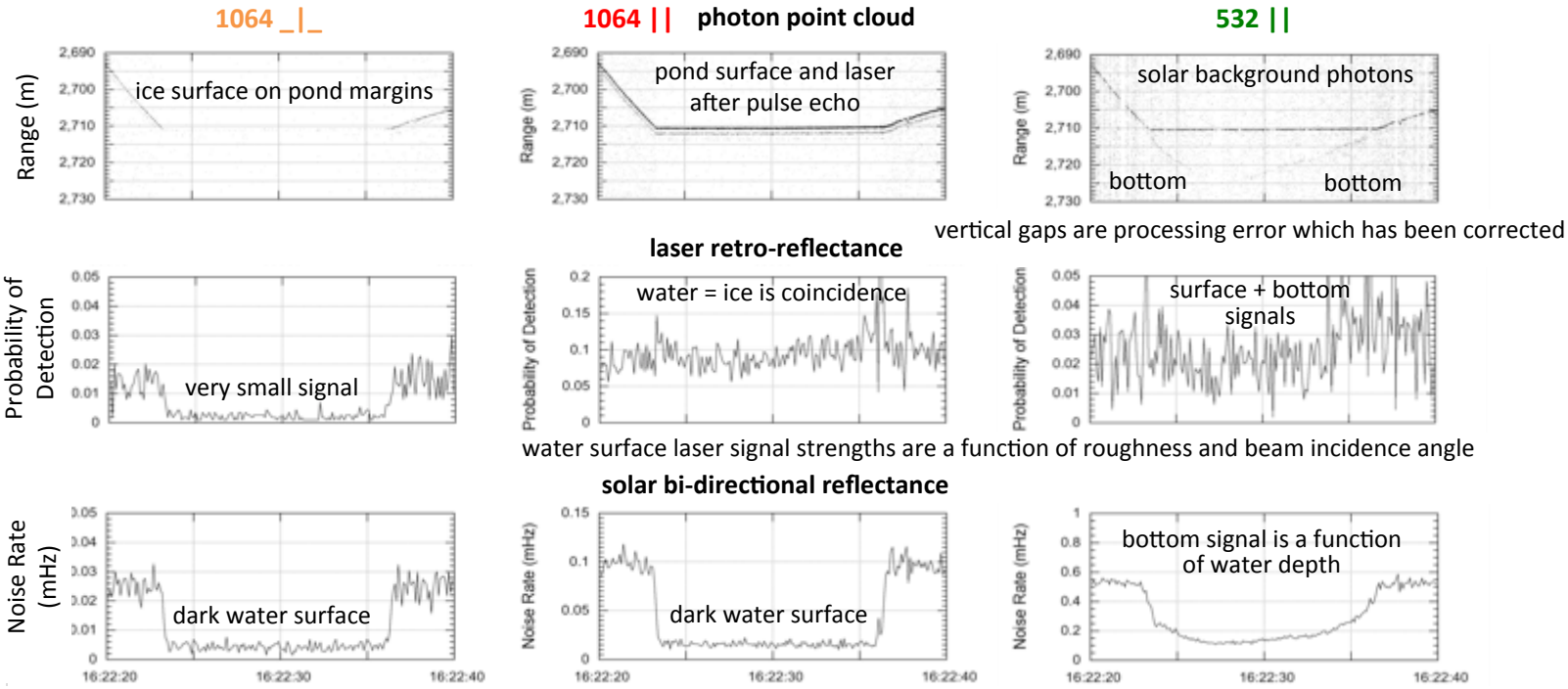

PD and noise rate are computed at 10 Hz (~ 10 m) and smoothed with running 5 bin average

532 _|_ not shown because melt water is so clear there is no column volume scattering. Also the bottom signal is absent perhaps because its surface is glassy and specular.

NW Greenland coastal ablation zone melt pond; frame camera image

4 km long frame camera image composite

Variations in Laser Retro-reflectance Signal Strengths are Sensitive to Scattering Properties
2009 Lake Erie Ice Cover and Open Water Photon Point Clouds

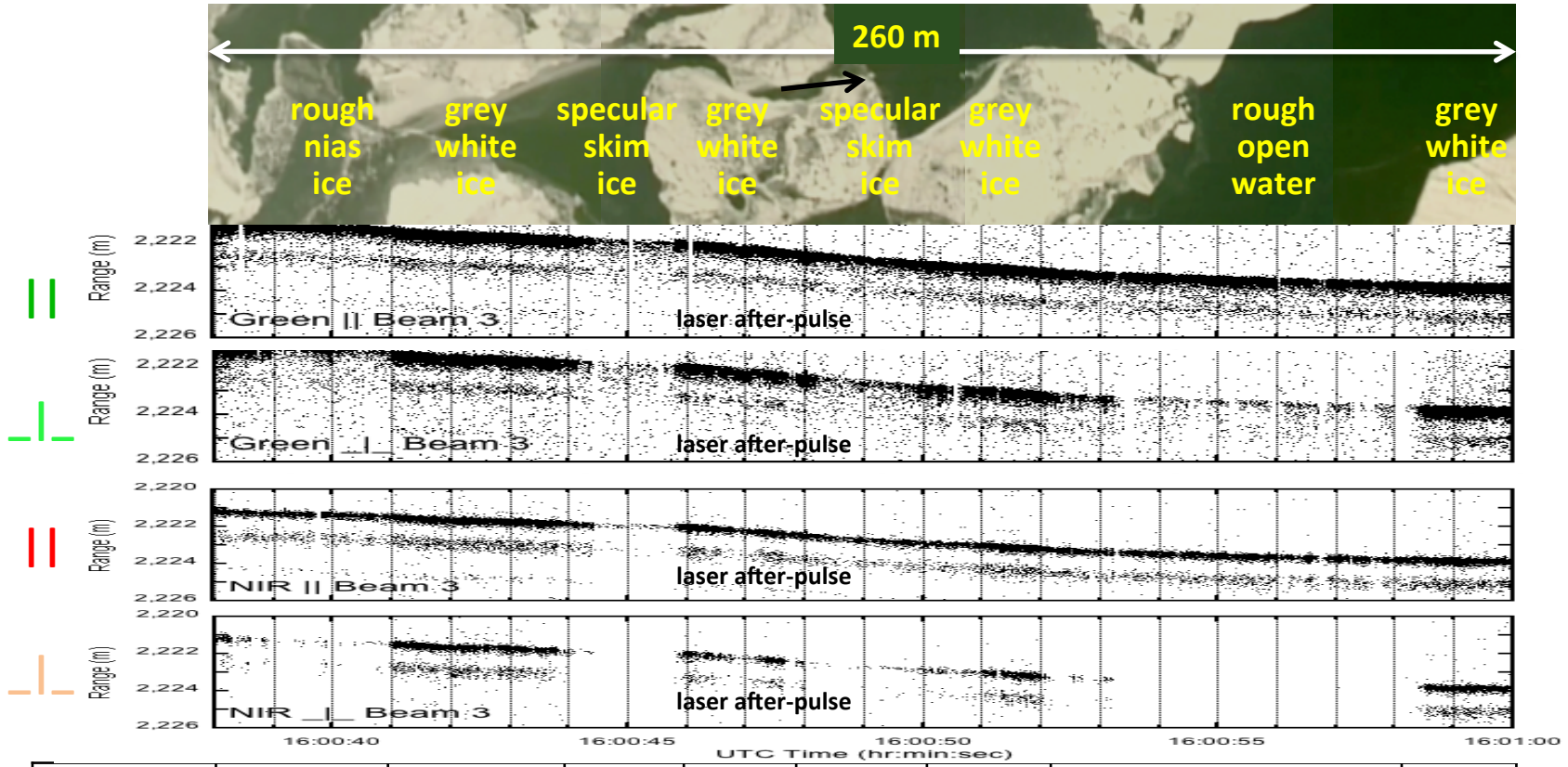

Green ||	S + V	S + V	< S + V	S + V	S + V	S + V	S + V	S + V
Green _|_	V	S + V	V	S + V	V	S + V	V	S + V
NIR ||	S	S	< S	S	S	S	S	S
NIR _|_		S		S		S		S

S = surface scattering. V = volume scattering. Increased _|_ signal is caused by increased multiple scattering.

The non-normal incidence angle to the smooth specular skim ice causes most surface scattering to be reflected away from the receiver. More surface signal is reflected to the receiver from the wind-roughened specular open water.

Aircraft roll effects on range not removed. After pulse strength in 2015 is smaller than in this 2009 data.

Variations in Laser Retro-reflectance Signal Strengths are Sensitive to Scattering Properties
2009 Lake Erie Ice Cover and Open Water Probabilities of Detection

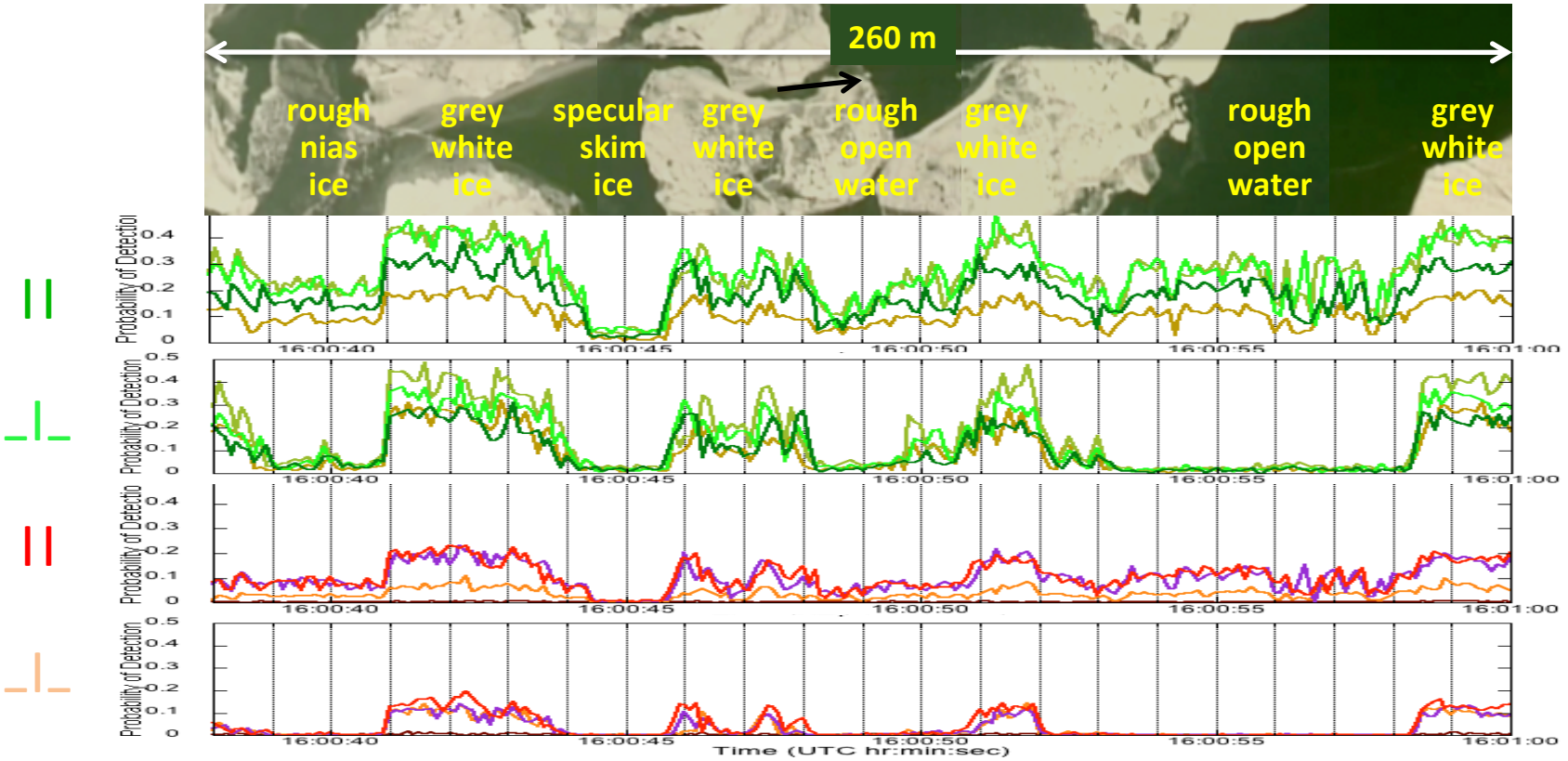

Green ||	S + V	S + V	< S + V	S + V	S + V	S + V	S + V	S + V
Green _|_	V	S + V	V	S + V	V	S + V	V	S + V
NIR ||	S	S	< S	S	S	S	S	S
NIR _|_		S		S		S		S

S = surface scattering. V = volume scattering. Increased _|_ signal is caused by increased multiple scattering.

The non-normal incidence angle to the smooth specular skim ice causes most surface scattering to be reflected away from the receiver. More surface signal is reflected to the receiver from the wind-roughened specular open water.

These PD values, using the sum of main pulse and after pulse photons, are computed at 10 Hz then smoothed to 2 Hz.

PRNR Folder Contents

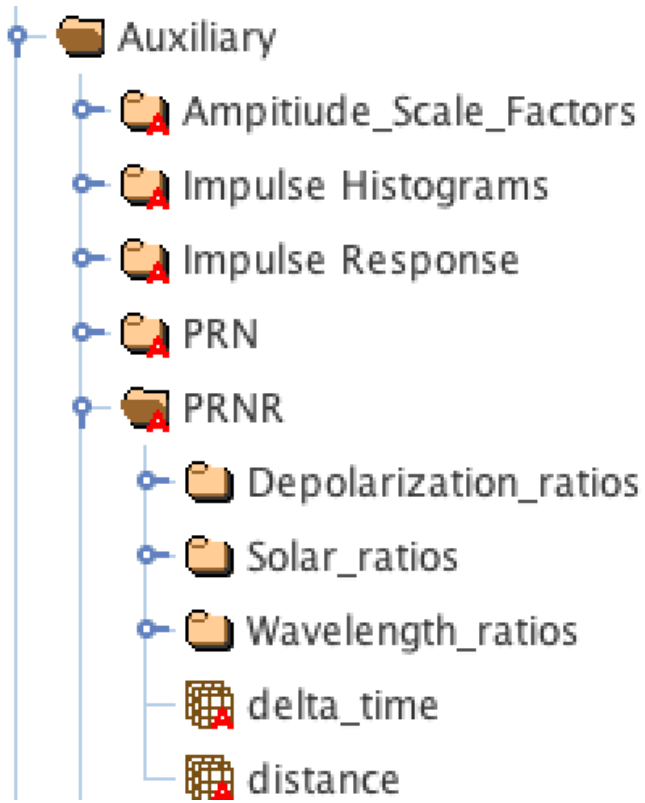

Ratios between PRN parameters are provided that provide information about surface reflectance and light scattering properties.

- Ratios in the Depolarization folder are equal to the number of perpendicular photons divided by the parallel photons. For the laser signal photons (PD ratios) it is a measure of the amount of surface and volume multiple scattering. For the solar background noise rate (NR ratios) it is a measure of the degree to which randomly polarized sunlight is polarized by reflectance from specular surfaces.
- Ratios in the Solar folder are equal to the signal photon PD (laser "hot spot" retro-reflectance) divided by the background noise rate (solar bi-directional reflectance). These are sensitive to increasing slope (changing the solar incidence angle) and increasing roughness (increasing the solar shadow fraction).
- Ratios in the Wavelength folder are equal to the number of near infrared photons divided by the number of green photons, for both the laser PD and solar NR. They are sensitive to the composition of the surface (e.g. snow, firn, ice, dirty ice) because of wavelength-dependent reflectance differences.

Delta_time is the offset in seconds with respect to midnight of that day. Seconds since the first GPS epoch = delta_time + [604,800 sec/week x start_gpsweek (in /ancillary_data)] + [86,400 sec/day x day of week]

Distance is an approximate distance along the profile assuming a nominal aircraft ground speed of 105 m/sec.

Variations in Laser Retro-reflectance Signal Strengths are Sensitive to Scattering Properties
2009 Lake Erie Ice Cover and Open Water Depolarization Ratios

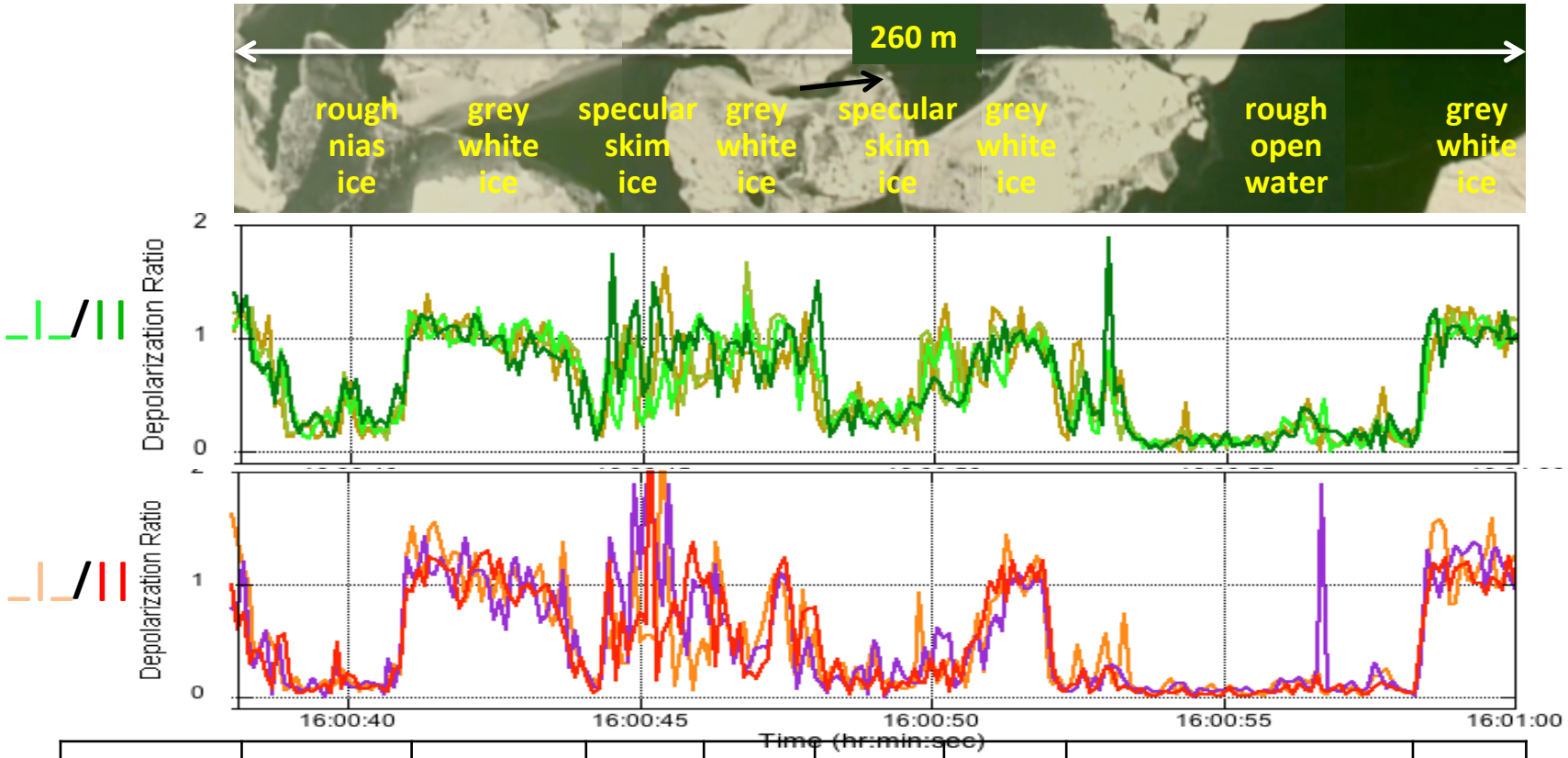

Green ||	S + V	S + V	< S + V	S + V	S + V	S + V	S + V	S + V
Green _|_	V	S + V	V	S + V	V	S + V	V	S + V
NIR ||	S	S	< S	S	S	S	S	S
NIR _|_		S		S		S		S

S = surface scattering. V = volume scattering. Increased _|_ signal is caused by increased multiple scattering.

The non-normal incidence angle to the smooth specular skim ice causes most surface scattering to be reflected away from the receiver. More surface signal is reflected to the receiver from the wind-roughened specular open water.

These ratios, using the sum of main pulse and after pulse photons, are computed using the smoothed 2 Hz PD values.

Auxiliary Folder Contents

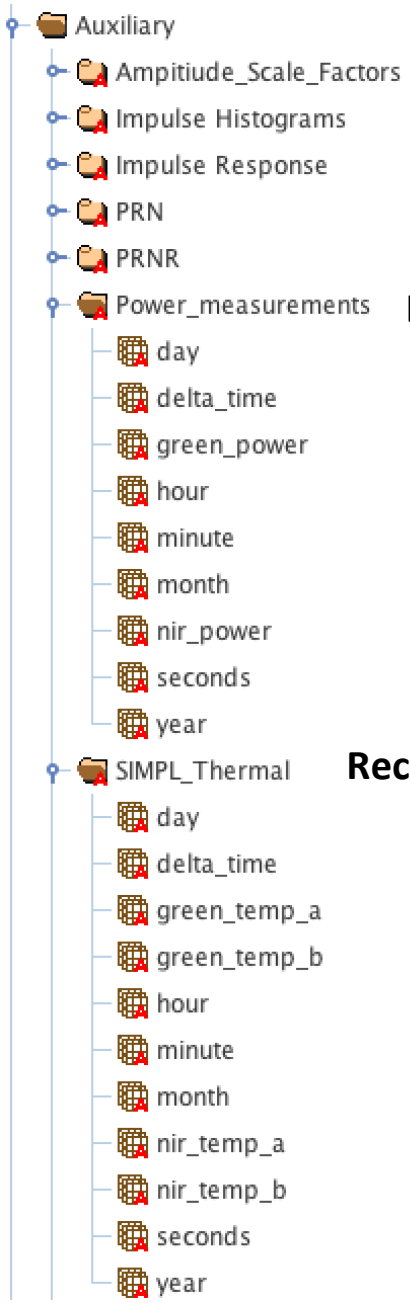

Two instrument status parameters were monitored through the duration of each flight. They may provide constraints for future modeling of instrument performance.

Laser output power time series

These time series are for the entire flight, not just the portion associated with an individual granule. The delta_time is given as the elapsed seconds since the first data point in the granule. Therefore power and thermal times that occur before the start of the granule will be negative numbers. Delta_time is the offset with respect to the GPS reference seconds given in /ancillary_data/gps_sec_offset. GPS Time (seconds since the first GPS epoch) = delta_time + gps_sec_offset.

Receiver filter block temperature time series

Instrument Monitoring for Signal Amplitude Calibration

Laser transmit powers and receiver spectral filter block temperatures

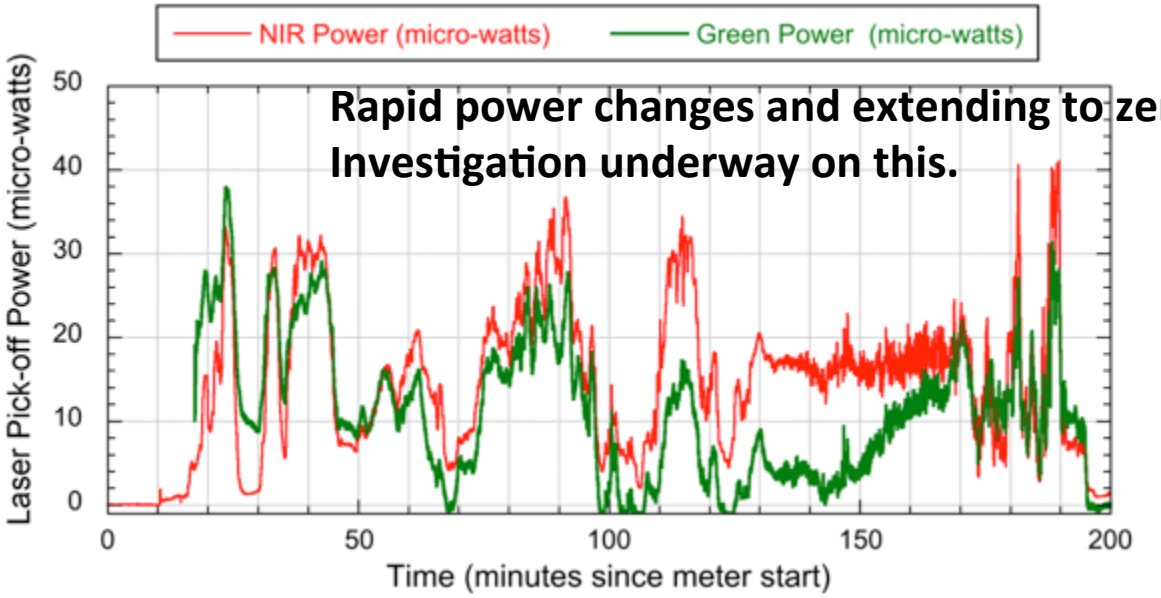

Rapid power changes and extending to zero are not understood. Investigation underway on this.

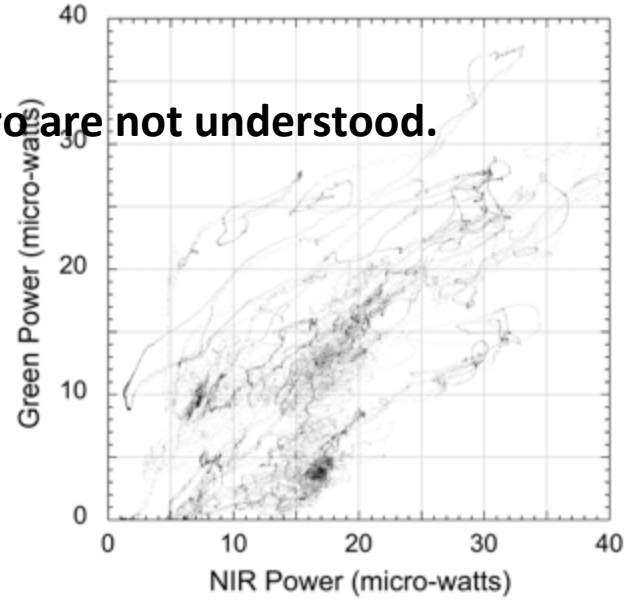

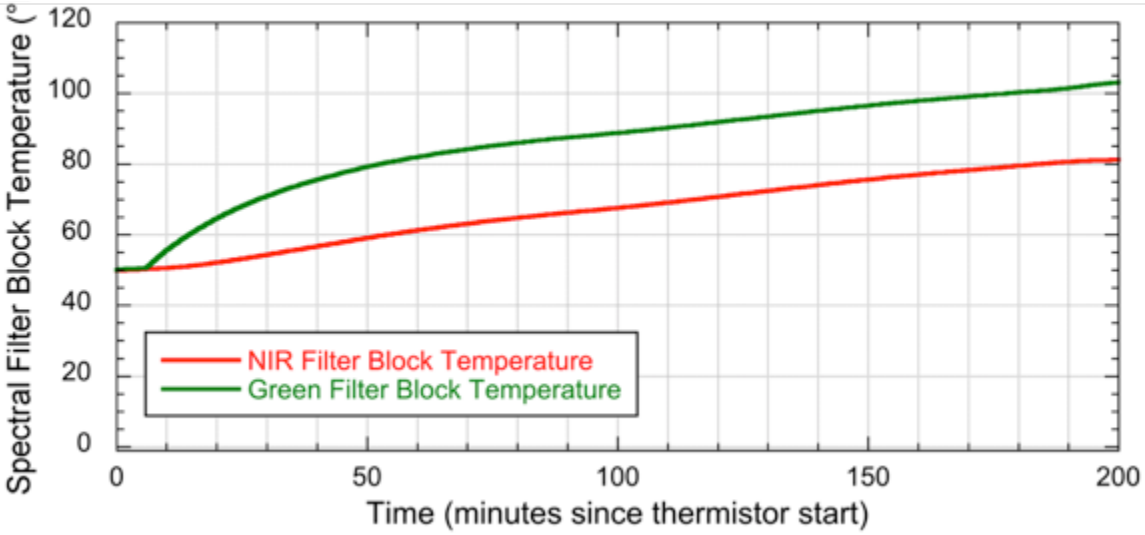

Features of note:

- Positive correlation between NIR and Green Tx powers but less consistent than expected. Need to assess why.
- Filter block temperature does not stabilize; not expected. On-off deadband switch not working? Need to assess effect on receiver throughput.

Release 5 Data Product Documentation and Instrument Description

SIMPL Instrument Description

March 30, 2016
Document Version 1.1

Transceiver Instrument Design

SIMPL uses an off-axis parabola optical design with the transmitter and receiver sharing the optical bench and primary and secondary mirrors. This design provides:

- stable laser footprint to receiver field of view alignment
- co-aligned NIR and green transmit beams
- co-incident NIR and green footprints

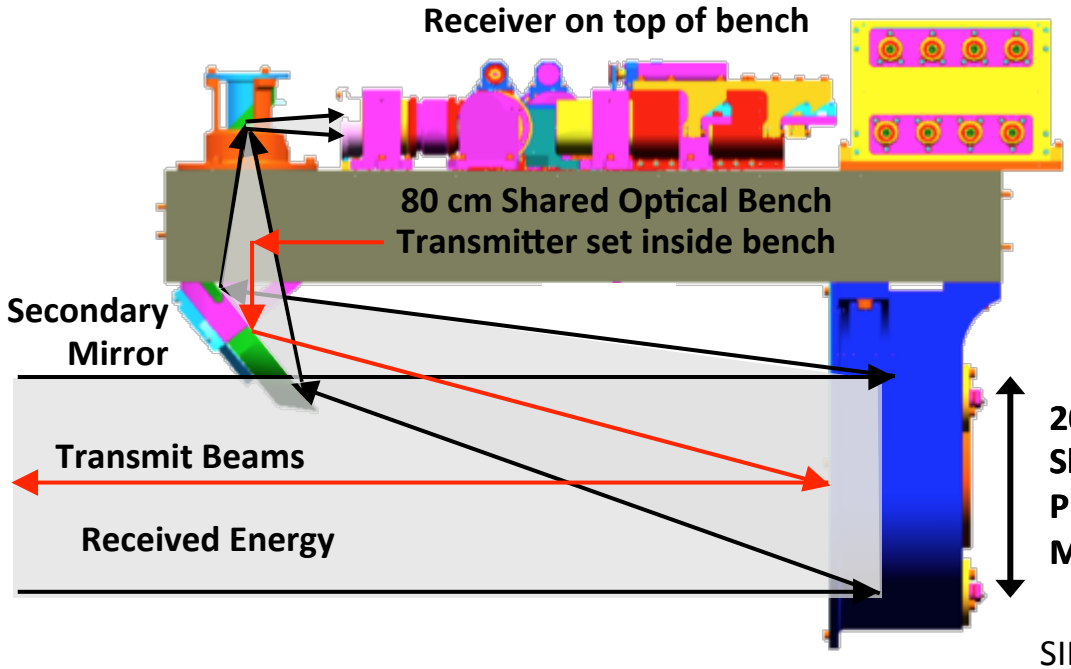

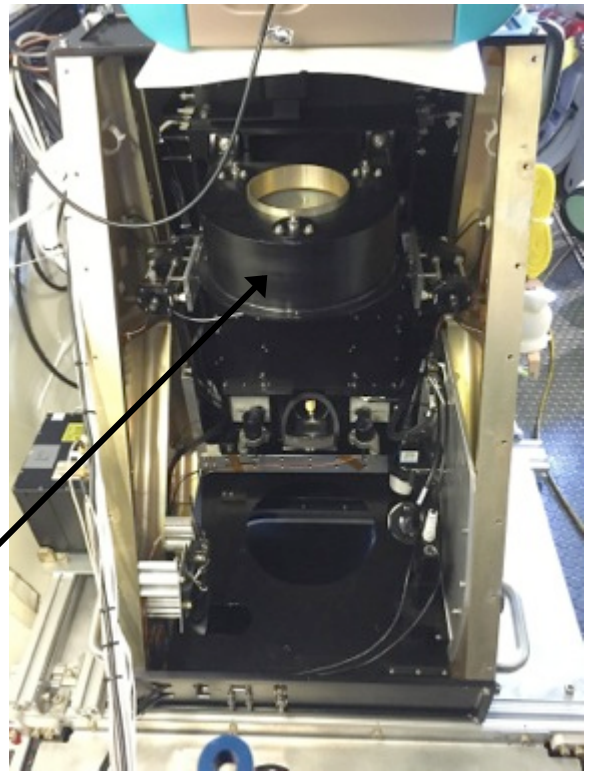

SIMPL optical bench inside its mounting frame (gold) installed in the Langley King Air. The instrument is fully enclosed with panels during operation.

Transmitter Components and Optical Path

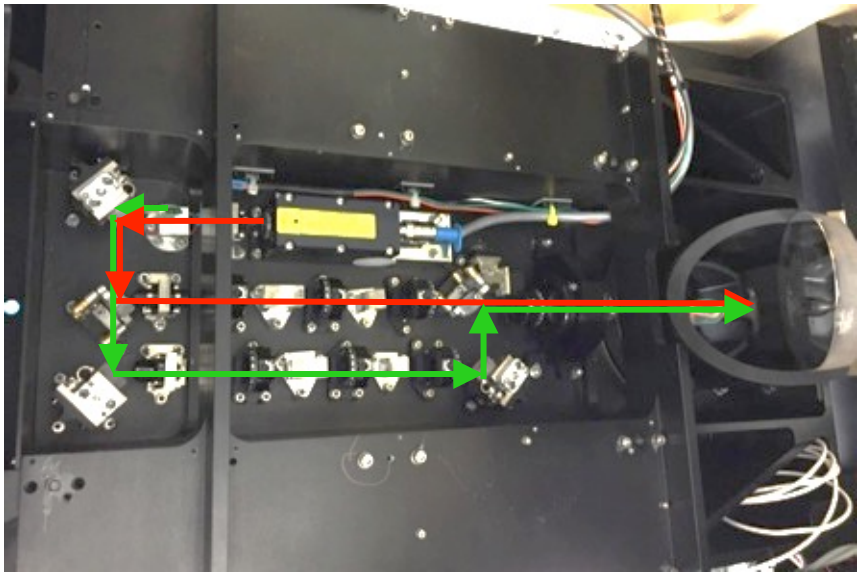

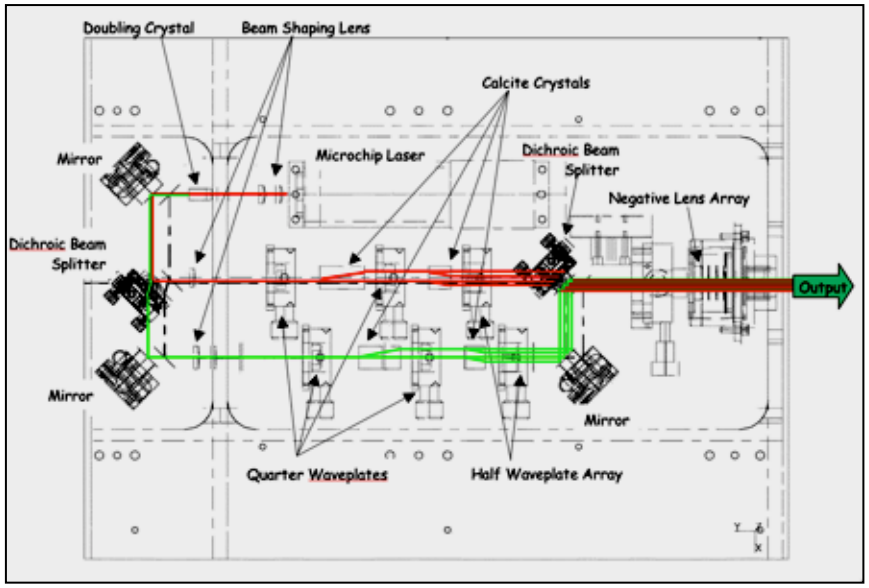

SIMPL utilizes a 1064 nm Teem Photonics (model SNP-08E-OEM) microchip laser that is passively Q-switched with a pulse repetition frequency (PRF) at ~11 kHz and ~6 µJ of output pulse energy. The pulse has a width of 1 nsec FWHM and a Gaussian beam profile. Using beam shaping lenses the 1064 nm output pulses are focused into a second harmonic frequency doubling crystal in which a portion of the transmit energy is converted to 532 nm. Temperature control of the crystal determines doubling efficiency defining the proportional amount of 164 nm and 532 nm power. The minimum and maximum set point of 35° C and 65° C correspond to 38% and 15% conversion efficiency, respectively. A dichroic beam splitter divides the two colors into separate optical paths that begin with beam shaping lenses to establish the beam divergence. Laboratory measurements using the original SIMPL laser determined the divergence was 130 urad for both colors. A new microchip laser was used during the 2015 Greenland campaign. That beam divergence has not been measured yet and could differ. After the beam shaping lenses a portion of the energy on each path is reflected vertically and exits the transmitter enclosure through three apertures. This light triggers the start pulse detector, is used for impulse response pulse shape measurements and to monitor the output laser power. On each optical path a sequence of waveplates and birefringent calcite crystals produce four beams which all have the same polarization plane. The first quarter waveplate circularizes the plane polarized transmit beam which is then split by the first calcite crystal into parallel and perpendicular components forming two beams. The physical separation of the beams is defined by the calcite crystal length. The second quarter waveplate circularizes those beams and then the second, shorter calcite crystal splits the two beams into the two polarization components, forming four beams. The half waveplate rotates two of the beams polarization planes by 90° so that all beams have the same polarization plane oriented perpendicular to the optical bench. A second dichroic beam optic recombines the two colors and precision alignment of the optical components produces co-aligned 1064 nm and 532 nm beams. A negative lens array establishes the 2.1 mrad beam-to-beam divergence. A polarizing beam splitter is used as a final step to ensure ≥ 100:1 plane-parallel polarization purity. Anthony Yu at Goddard Space Flight Center designed and implemented the laser transmitter.

Folding Mirrors and Optical Path

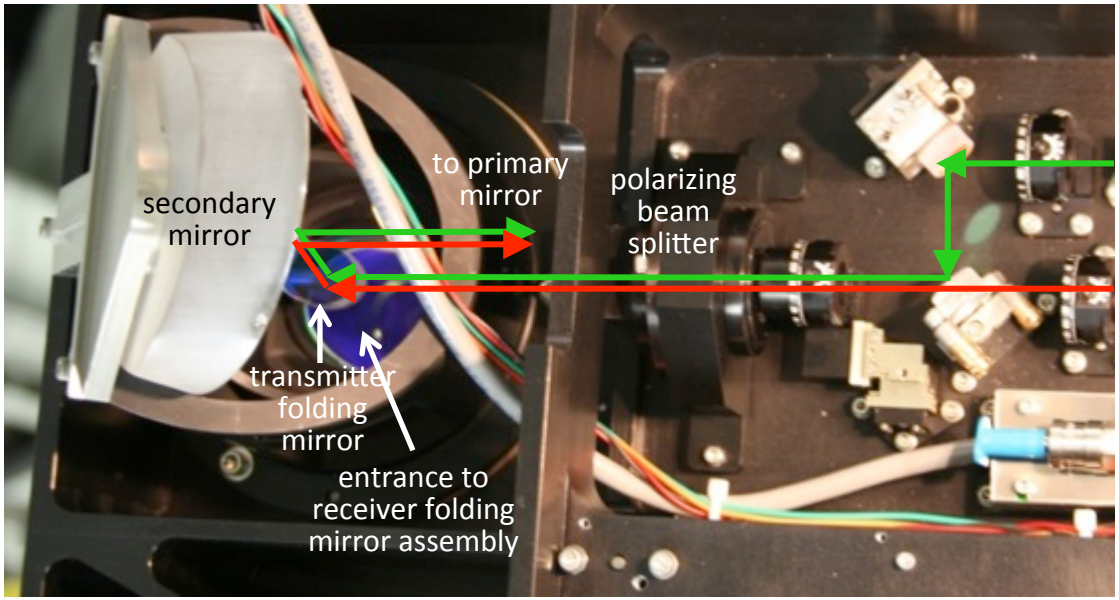

After passing through the polarizing beam splitter the transmit beams reflect off of a small folding mirror. The folding mirror directs the beams perpendicularly to the secondary mirror which reflects the beams to the 20 cm diameter primary mirror. That mirror reflects the beams at nadir to the surface. Upon exit from the instrument the beams are overlapping with a combined diameter of 70 mm and 5 mm beam-to-beam separation. The Nominal Ocular Hazard Distance of the combined beams and colors is 0 m and is therefore eye safe. The diverging beams become fully separated at a distance of 23 m.

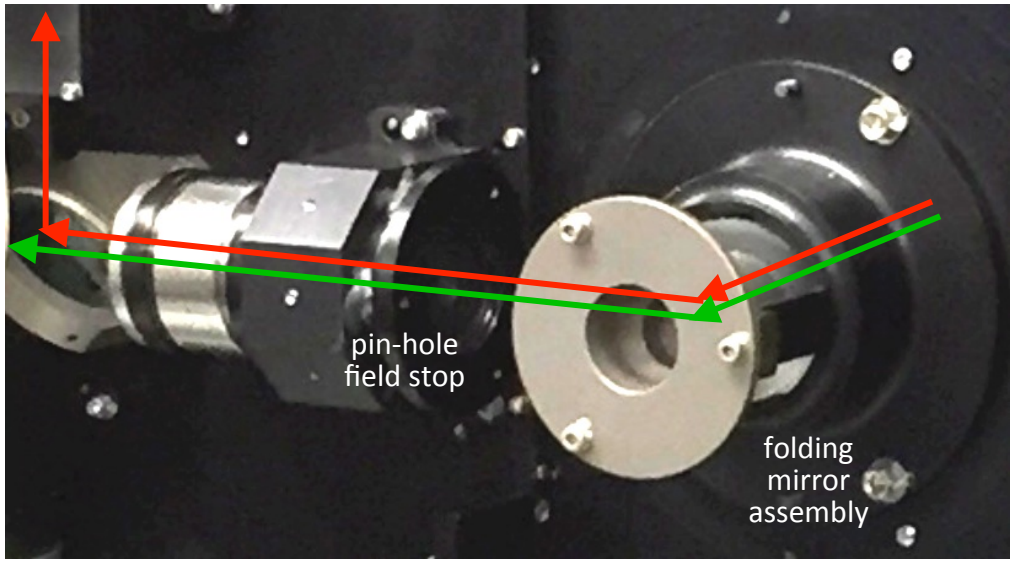

Upon entry into the instrument's 20 cm aperture a small portion of the returned laser energy is blocked by the back of the secondary mirror assembly. The remaining energy is reflected by the primary mirror to the secondary mirror where it reflects perpendicularly to the optical bench. A portion of the light is intercepted by the transmit folding mirror and is back-reflected into the transmitter optics but the signal strength is too weak to effect the laser performance. The majority of the light passes through a hole in the optical bench and enters a folding mirror assembly that reflects the light 90° so that the path is parallel to the optical bench. The beams are directed to a pin-hole field stop.

Transmit Echo Pulse, Start Pulse Detector and Power Meter

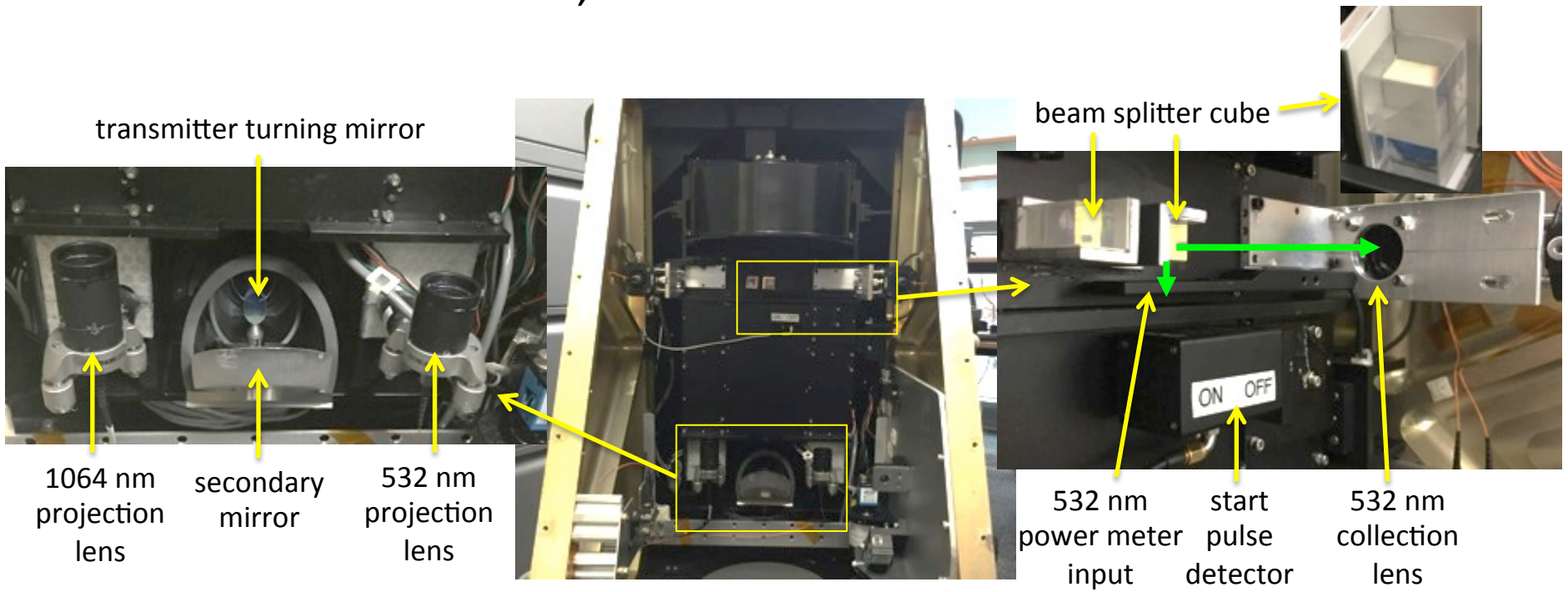

The laser pulse energy directed vertically out of the transmitter enclosure through three apertures is used for three purposes. Light enters a start pulse detector to provide pulse events to the receiver electronics that are used as the starting time of the photon round-trip travel time measurement. For each wavelength light enters a beam splitter cube that directs part of the light to a Transmit Echo Pulse (TEP) collection lens and the remainder to a power meter. The TEP optics are used to record the instrument impulse response pulse shape which is the convolution of the transmit pulse shape and the receiver pulse broadening. Fibers transmit the two colors through couplers to 38 m fiber spools which delay the pulses to separate them in time from internal scattered light signals. The delay fibers are coupled to fibers that transmit the pulses to projection lenses that disperse the light onto the primary mirror. This light follows the receive path to record the impulse responses using the same optics and electronics as the pulses reflected from the surface. Deconvolution of the impulse response from the surface return provides a measure of pulse broadening due to surface roughness, slope and penetration. The other portion of the light divided by the beam splitter is directed to a Thorlab power meter that records transmit power variability at 532 nm and 1064 nm. Anthony Yu at Goddard Space Flight Center designed and implemented the TEP optical assemblies.

532 nm and 1064 nm fiber spools to delay TEP

Receiver Components and Optical Path

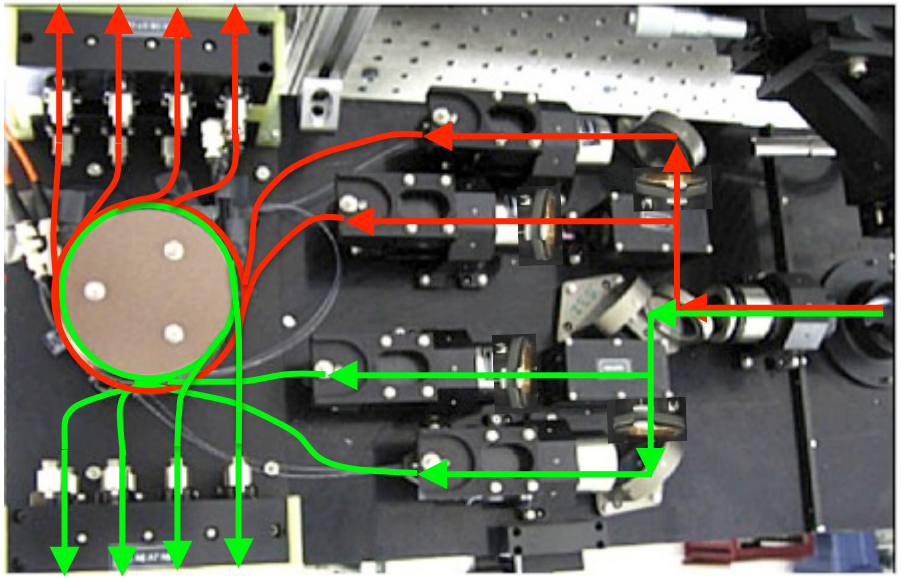

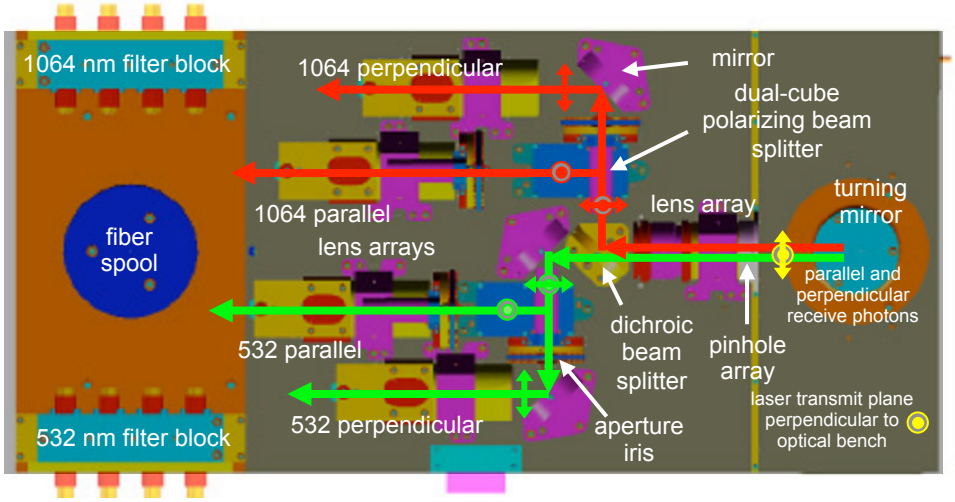

The field stop consists of four pin holes that define a 233 urad field of view for each beam. The small FOVs are used to spatially reject solar background photons. A lens array follows that collimates the incoming beams and a dichroic beam splitter divides the two colors into separate optical paths. On each path a double stack of polarizing beam splitter cubes separates the return energy into photons with polarization states that are parallel and perpendicular to the plane-parallel polarized transmit beams. The four color + polarization modes each pass through a mechanical iris that can be used to attenuate the beam energy (the irises were not installed on the bench at the time of the photo; insets have been added to show their location). Each iris opening size is set independently. As they are closed the attenuate the outer beams more rapidly then the inner beams. The irises were set to be fully open for all 2015 flights. Lens array assemblies for each of the four modes focus the beams into four fibers which have a 0.22 numerical aperture and 100 micron stepped index core size. Using a spool to reduce bending the fibers are coupled to 1064 nm and 532 nm filter blocks each of which consist of eight narrow-band spectral filter assemblies to reject out-of-band solar background photons. The filter assemblies are temperature controlled with dead-band heaters to maintain stable band pass wavelengths. Two thermistors are installed on each block to record the temperatures at two locations using a four-channel Hobo data logger. One 1064 nm block thermistor was not operating during 2015. The data showed that the block temperatures slowly increased throughout the duration of the flights rather than being stabilized at a constant temperature. The cause is not known. What, if any, impact the non-constant temperature had on receiver throughput is not known and will be evaluated. On exit from the filter blocks 16 fibers, which have a 0.37 numerical aperture and 200 micron stepped index core size, transmit the signals to four single-photon-counting-module (SPCM) quad detectors in an adjacent instrument rack. The four signals for a beam are directed to one of the quad detector modules. Yunhui Zheng and Tim Huss at Sigma Space Corp. were the lead optical and mechanical engineers who designed and integrated the receiver under the direction of Philip Dabney at Goddard Space Flight Center, the SIMPL instrument scientist and system engineer.

Electronics Rack

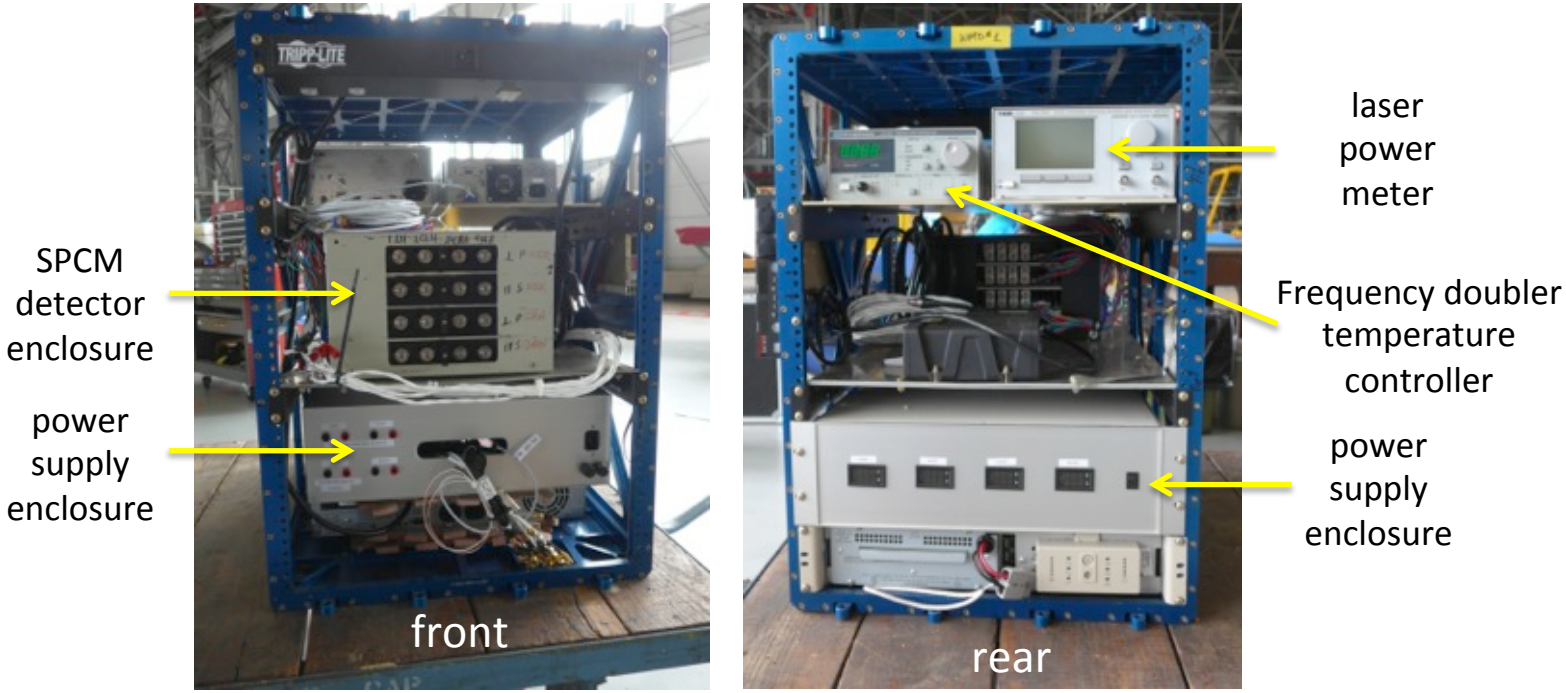

The 19 inch wide, half-height electronics rack is installed behind the SIMPL transceiver. The rack houses an enclosure containing the four SPCM quad detector assemblies which are silicon avalanche-photodiode (SI:APD) devices manufactured by Intevac. The SPCM detection quantum efficiency is in the range 50 to 60% at 532 nm and 1.6 to 2.3% at 1064 nm. The Intevac SPCMs were the only photon counting detectors available at the time of SIMPL's development with sensitivity in the NIR so their use was required. Each detector in an assembly receives signals from one of the four channels on a beam. Upon detection of a photon the detectors generate an electrical pulse that is transmitted to four P7889 event timer interface boards in the command and data handling rack. The electronics rack also houses a power supply enclosure, Lightwave laser power meter and a Thorlab doubling crystal temperature controller. The maximum and minimum conversion efficiencies used were 38% and 15%, at 35° C and 65° C, respectively. Intermediate temperatures were also used. There is no-inflight knowledge of the surface return PD. Doubler temperature and aircraft altitude were planned pre-flight based on the nominal NIR and green reflectances of the target surfaces with the goal of achieving PDs in the range 4% to 10%. This was the goal in order to have an adequate density of return photons while not introducing a large first photon range bias due to detector saturation. The power supply enclosure contains three DC power supplies (Acopian Gold Box High Performance linear AC-DC), a laser fire start-pulse discriminator, two ASRC Federal transistor–transistor logic (TTL) fan-out boards and front panel mounted voltage and current meters. The discriminator takes as input the signal from the laser fire start pulse detector. One fan-out board takes this discriminator output and produces duplicate laser fire pulses that go to the four individual P7889 boards. The other fan-out board distributes the GPS 1 pulse per second signal to the four interface boards. Philip Dabney and Kurt Rush at Goddard Space Flight Center designed and integrated the electronics.

Command and Data Handling Rack

front

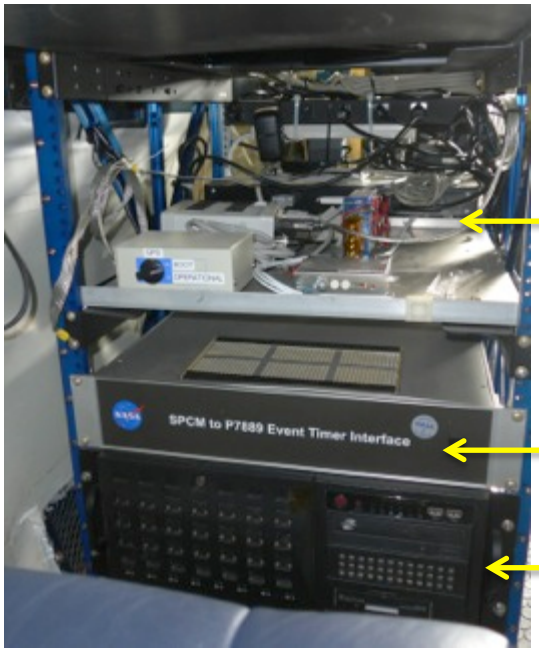

Laser controller and power supply and GPS totally accurate clock (TAC) and controller

P7889 event timer Interface boards enclosure

custom C&DH computer and RAID drives

front

The 19 inch wide, half-height command and data handling (C&DH) rack is installed in front of the SIMPL transceiver. The rack houses the enclosure that contains four P7889 event timer interface boards. Each board times the arrival of the laser fire start pulses, the GPS once per second pulses (from the TTL fan-out boards) and the detected photon pulses with 0.1 nsec (1.5 cm) resolution. Each board times the photon events for the four channels on a beam (1064 nm parallel and perpendicular and 532 nm parallel and perpendicular). The relative arrival times of all events are recorded based on the CPU clock frequency. Absolute time is recorded for the start and end of each file taken from the CPU clock which is synched to GPS time using a totally accurate clock which receives input from a dual-frequency GPS antennae mounted on the top of the aircraft fuselage. The computer issues commands to the instrumentation and stores the event arrival times on RAID drives. The rack also houses the CPU keyboard and screen and the laser controller and power supply. A Lenova Windows laptop installed on the top of the rack is used to run the Applanix Pos AV and power meter software. It also records the frame camera images. Susan Valett at Goddard Space Flight Center, the SIMPL software engineer, developed the interface to the P7889 cards, the flight control and data collection software and the ground processing software. Elizabeth Timmons at Goddard Space Flight Center integrated the laptop and associated software.

SIMPL Greenland 2015 Campaign

Release 5 Data Product Documentation and Instrument Description

Ancillary Data: Applanix, Frame Camera and Hyperspectral Data

March 30, 2016
Document Version 1.1

Ancillary Instrumentation

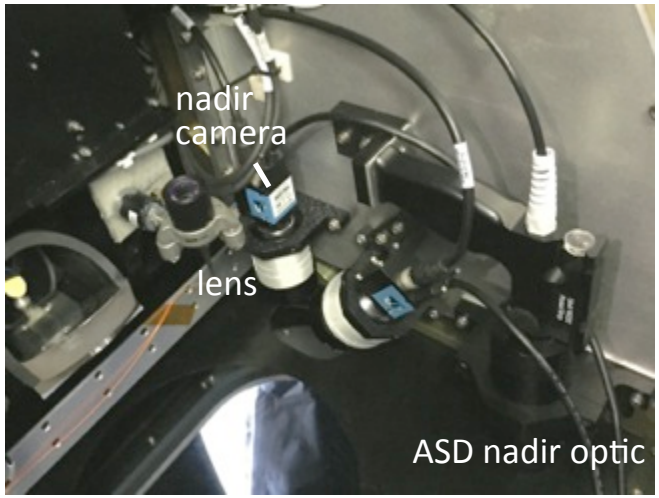

Flown on NASA Langley King Air with SIMPL

Applanix POS/AV 610 IMU+GPS

- Recorded SIMPL position and attitude data used in geolocation
- Mounted adjacent to SIMPL using same seat track rails for stable alignment
- Provided and installed by NASA Ames Research Center

Nadir frame camera

- Thorlabs DCU223C color CCD Camera, 1024 x 768 Resolution
- Fuji Photo Optical Co. Lens 678437, 1:1.4/50
- Image taken once a second controlled by GPS to synch with SIMPL
- Attached to SIMPL mounting frame for stable alignment
- Second oblique-angle camera for stereo imaging installed but not used (FOV blocked)

Two ASD FieldSpec 4 Spectroradiometer profilers – Chris Crawford, GSFC

- Fiber-coupled nadir and zenith viewing with 1° and cosine reflector fore-optics, respectively
- Nadir optic attached to SIMPL mounting frame for stable alignment

Flown on Dynamic Aviation King Air

JPL AVIRIS-NG Hyperspectral Imager – Rob Green, PI

- Flown at higher altitude than SIMPL
- Followed Langley King Air flight path trailing by 15 to 20 min

Nadir Color Camera

- Thorlabs DCU223C color CCD Camera
- Fuji Photo Optical Co. Lens 678437, 1:1.4/50
- Image taken once a second
- Attached to SIMPL mounting frame for stable alignment
- File name is time synched using GPS 1 PPS

  All July flights EDT local time = GPS – 4 hr; reset for August flights to GPS – 0 hr

SIMPL 18 m beam spread at 2,500 m

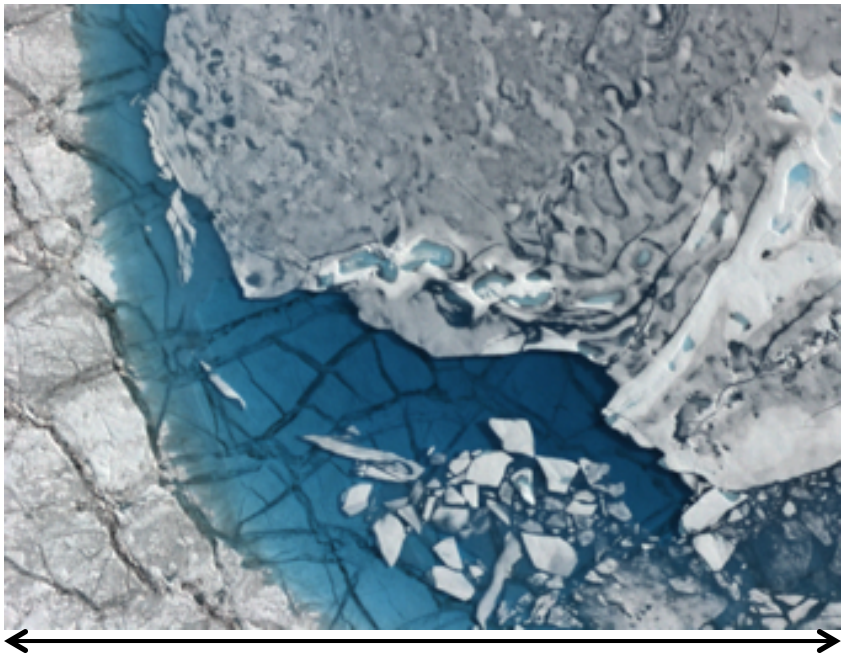

W = 372 m at 2,500 m

Camera
1680 horizontal pixels; 1200 vertical pixels
Pixel Size 4.40E-06 m
Chip size - V 5.28E-03 m; W 7.39E-03 m
Lens
Focal length = 5.00E-02 m
FOV – V = 1.06E-01 radians; 6.04E+00 deg
FOV – W = 1.48E-01 radians; 8.46E+00 deg
At nominal 2,500 m flight altitude
Frame size – V = 264 m
Frame size – W = 372 m
At nominal 100 m/sec ground speed
Frame 0verlap – V = 2.6x
Resolution ~ 0.5 m
0.2 m pixel with color re-sampling blur and optics MTF
V = in-track W = cross-track

Laser footprints are within the frame but location varies with altitude because the camera and lens were not bore-sighted. Can be established using altimetry profile matching to image features.

AVIRIS vs. Frame Camera Comparison

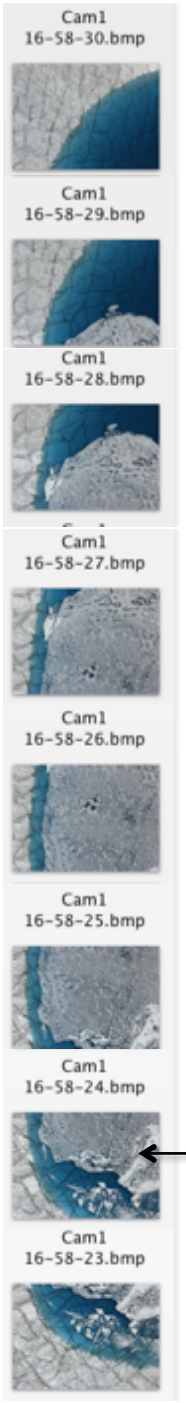

Two potential sources of confusion:

- AVIRIS King Air trailed SIMPL King Air by about 15 to 20 minutes.
- SIMPL King Air sometimes made turns to cross over melt-ponds while King Air flew straight

Frame Camera
mounted inside SIMPL

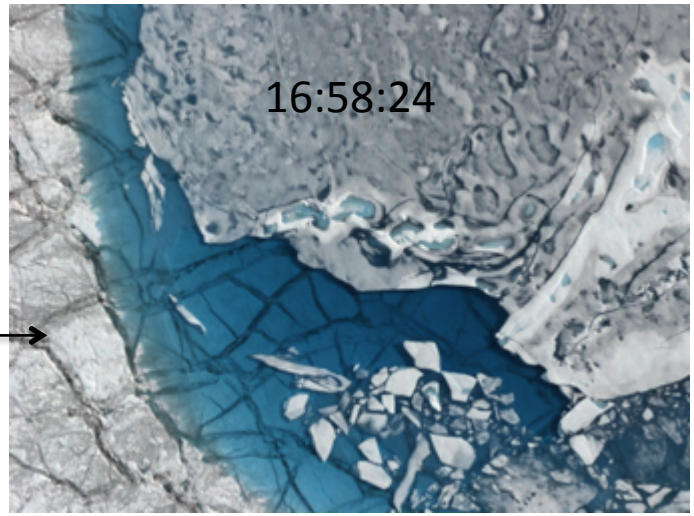

Representative Frame Camera Images

Melting Pack Ice in Nares Strait

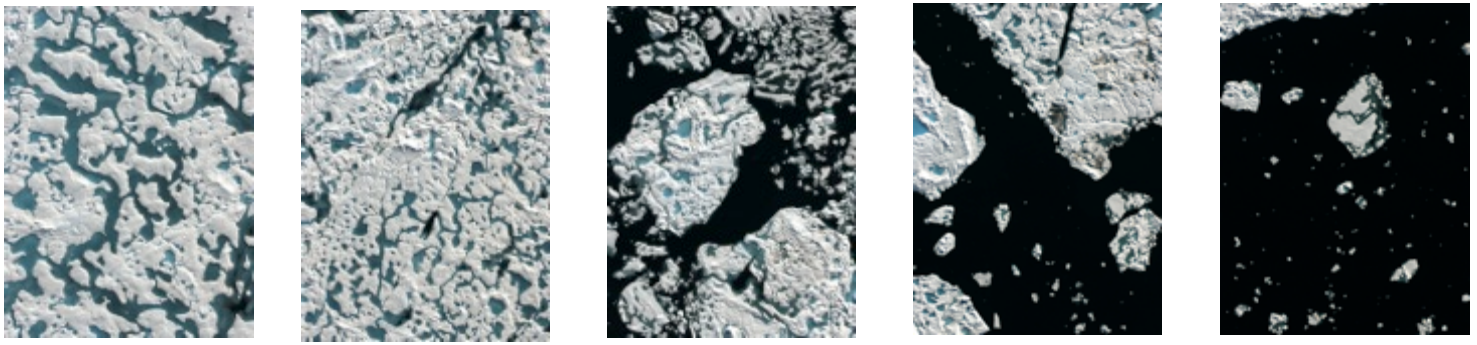

~ 0.4 km
altitude
dependent

High Elevation Interior Accumulation Zone

Interior and costal images are brightness and contrast enhanced to emphasize surface features

Low Elevation Coastal Ablation Zone

Circular dark blotch in lower right is dust speck on inside of lens (cleaned off for later flights)

Sequential Frame Camera Images

Images are brightness and contrast enhanced to emphasize surface features

Sea Ice North of Ellesmere, August 7, 2015

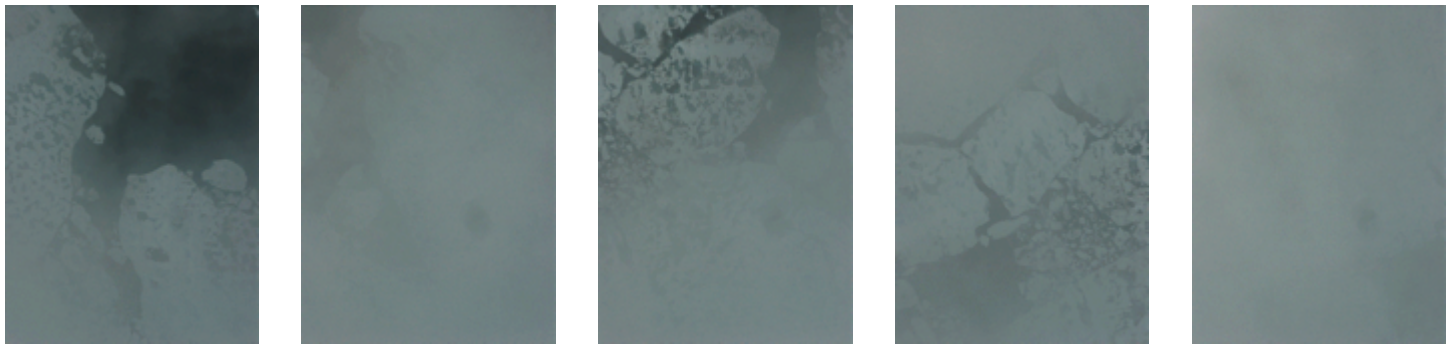

Flight was mostly cloudy below the plane and at times water condensed on window exterior (no surface signal) with rare views of surface (weak signal). Also cloudy above plane so solar illumination was weak and diffuse.

Tarmac Pass in front of Thule Hangers

~ 0.3 km altitude dependent

SIMPL – Hyperspectral ASD – Camera Boresight Test in Thule Hanger

NADIR VIEW INSIDE PLANE

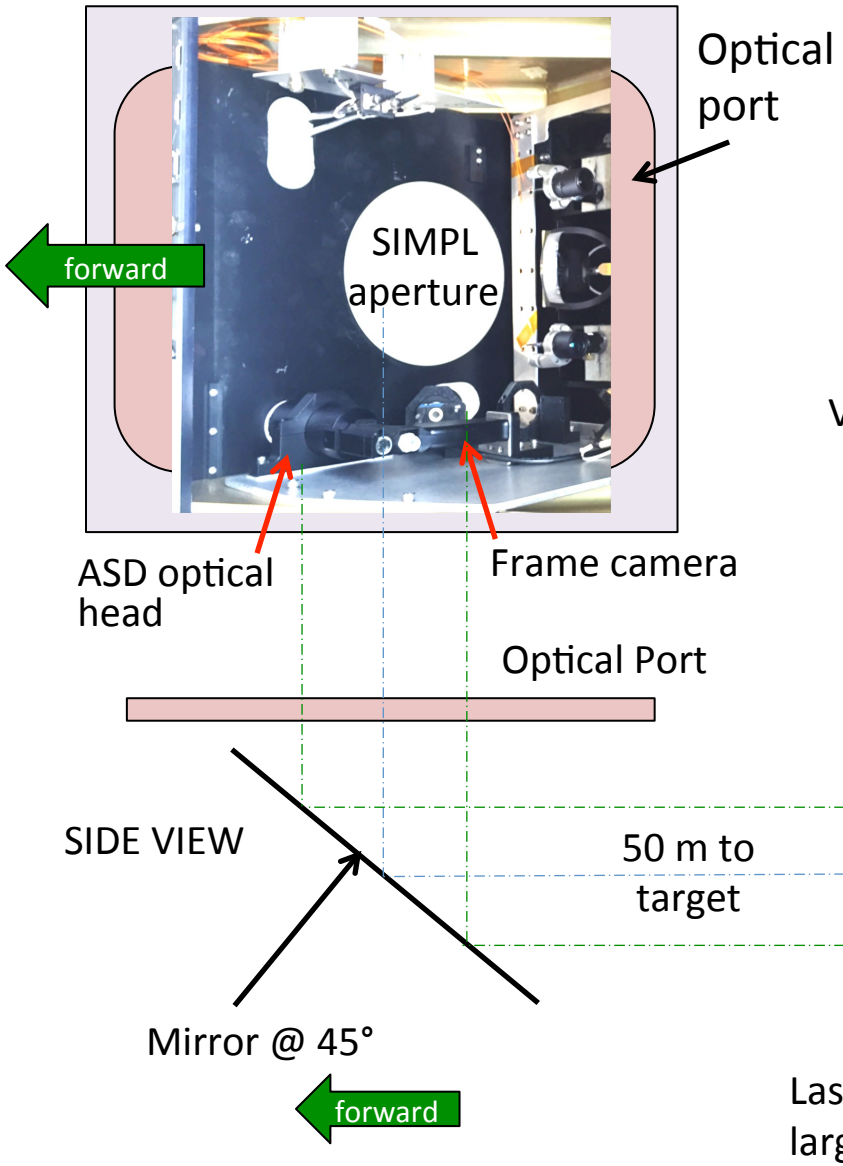

- SIMPL laser spots (green) are at trailing edge of ASD optic 1° FOV (yellow; 45 m @ 2,500 m)
- Forward flight ensures the two tracks sample the same profile

- Location of maximum ASD signal from back-projected LED
- LED pointing oriented to maximize brightness in camera image to align FOV axes

HORIZONTAL VIEW TO TARGET

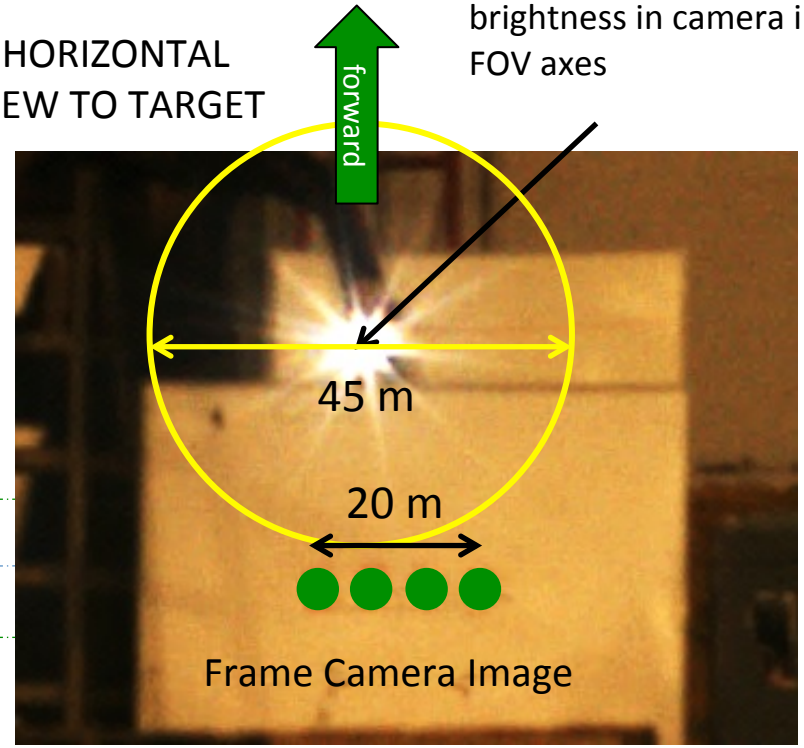

Laser spots (indicated by green circles) in the near-field are large relative to their spacing compared to on the ground

SIMPL Greenland 2015 Campaign

Release 5 Data Product Documentation and Instrument Description

References

March 30, 2016
Document Version 1.1

GODDARD SPACE FLIGHT CENTER

SIMPL Publications

Dabney, P., D. Harding, J. Abshire, T. Huss, G. Jodor, R. Machan, J. Marzouk, K. Rush, A. Seas, C. Shuman, X. Sun, S. Valett, A. Vasilyev, A. Yu, and Y. Zheng, 2010, "The Slope Imaging Multi-polarization Photon-counting Lidar: development and performance results," in Geoscience and Remote Sensing Symposium, 2010 IEEE International, 253-256, DOI10.1109/IGARSS.2010.5650862.

Harding, D., P. Dabney, S. Valett, A. Yu, A. Vasilyev and A. Kelly, 2011, "Airborne polarimetric, two-color laser altimeter measurements of lake ice cover: A pathfinder for NASA's ICESat-2 spaceflight mission", in Geoscience and Remote Sensing Symposium (IGARSS), 2011 IEEE International, 3598-3601, DOI 10.1109/IGARSS.2011.6050002.

Harding, D.J., P.W. Dabney and S. Valett, 2011, "Polarimetric, Two-Color, Photon-Counting Laser Altimeter Measurements of Forest Canopy Structure," Proceedings of 2011 International Symposium on Lidar and Radar Mapping: Technologies and Applications, SPIE - The International Society for Optical Engineering 06/2011; DOI:10.1117/12.913960

Yu, A.W., D.J. Harding and P. W. Dabney, 2016, "Laser transmitter design and performance for the slope imaging multi-polarization photon-counting lidar (SIMPL) instrument", Proc. SPIE 9726, Solid State Lasers XXV: Technology and Devices, 97260J (16 March 2016); doi: 10.1117/12.2213005.